Macromolecules

ARTICLE

pubs.acs.org/Macromolecules

# Synthesis of a Star Polymer Library with a Diverse Range of Highly Functionalized Macromolecular Architectures

Jing M. Ren, James T. Wiltshire, Anton Blencowe, and Greg G. Qiao*

Department of Chemical and Biomolecular Engineering, The University of Melbourne, Parkville, Victoria 3010, Australia

Supporting Information

**ABSTRACT:** An efficient and versatile synthetic route toward highly functionalized core cross-linked star (CCS) polymers with interesting structures and properties is presented using an alkyne CCS polymer as scaffold. The alkyne CCS polymer scaffold was initially prepared via an improved arm-first approach, through ring-opening polymerization (ROP) of 4,4′-bioxepanyl-7,7′-dione (BOD) with a poly(caprolactone-*b*-propargyl methacrylate) macroinitiator and stannous triflate ($Sn(OTf)_2$) catalyst. Highly functionalized fluorescent, saccharide and amphiphilic CCS polymers were synthesized by grafting the alkyne CCS polymer with the corresponding azido substituted compounds via copper catalyzed 1,3-dipolar azide−alkyne cycloaddition (CuAAC), 'click' chemistry. The resulting corona-functionalized CCS polymers were characterized via GPC, $^1$H NMR spectroscopic analysis and DLS. $^1$H NMR spectroscopic analysis revealed that the grafting efficiency (i.e., click efficiency) ranged from 10 to >99% and was highly dependent on the structure and functionality of the azido compounds. This equates to the grafting of 45 to 450 functional compounds onto the CCS polymer scaffolds corona. The results indicate that the click functionalization efficiency is closely related to the molecular size of the azido compounds. Other than size, factors including molecular structure, compatibility and synergistic driving forces, such as the formation of potential inclusion complexes, are also found to affect the functionalization efficiencies.

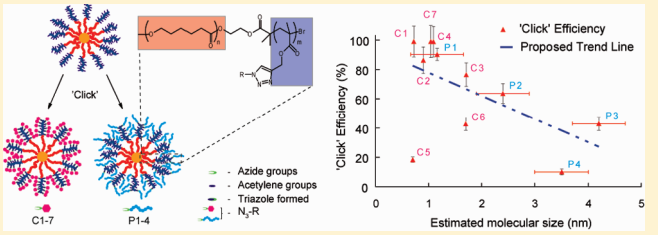


## INTRODUCTION

CCS polymers represent a unique type of three-dimensional (3D) macromolecular architecture consisting of a cross-linked core surrounded by a number of radiating arms, typically 10−100.[1] CCS polymers can often possess very high molecular weights, while still maintaining excellent solubility characteristics and low viscosities comparable to linear or branched polymers with lower molecular weights.[2] The distinctive rheological properties and 3D globular structure of CCS polymers has attracted significant interest and resulted in a number of potential applications, including polymer therapeutics and drug delivery,[3] cascade reaction catalysis,[4] microporous films,[5] and paint additives.[6]

Often, the design of CCS polymers carrying high desirable functionality and spatial control over their location is required to meet a diverse range of application needs. In particular, in polymer therapeutics, the synthesis of CCS polymers with high coronal functionality would be particularly beneficial for drug loading and conjugation of targeting moieties. Functional groups at the periphery of nanometer-sized drug carriers could facilitate drug encapsulation through either covalent bonding[7] or non-covalent (e.g., electrostatics[8]) interactions with complementary drugs such as peptides, proteins, nucleic acids and other therapeutic agents. Thus, an increased functional group density offers larger drug-loading potential. Moreover, a high number of reactive functional sites increases the chance of success in attachment of targeting moieties and binding agents to the carrier, which ultimately facilitates greater cell adhesion[9] and site-specific drug delivery.[10]

CCS polymers with high functionality, good structural control and narrow molecular weight distributions can be readily synthesized via controlled polymerization techniques,[11−15] and the arm-first approach.[16−18] Functional groups can be integrated into the periphery of CCS polymers via two discrete approaches; end-functional star polymers can be prepared from telechelic macroinitiators/macromonomers or block copolymer macroinitiators in which one block consists of a number of pendent functionalities. The drawback of the former is that the resulting star polymers possess a relatively low number of functionalities at the periphery, since the number of functional units is equal (restricted) to the number of arms. To overcome this, dendritic macroinitiators have been used to prepare CCS polymers,[19] leading to stars with up to 1100 peripheral functional groups. However, the preparation of dendritic macroinitiators generally involves multiple protection/deprotection steps, which require time and labor intensive synthetic protocols, especially considering that high dendron generation is required to achieve high functionality. In contrast, stepwise polymerization of functional monomers to yield block copolymer macroinitiators suitable for CCS polymer formation[20] is a more promising and synthetically

**Received:** February 8, 2011
**Revised:** March 23, 2011
**Published:** April 05, 2011

convenient route to introduce a large number of coronal functionalities. However, this synthetic route requires the preparation of desirable functional monomers before polymerization, which may be synthetically involved.[21] Furthermore, controlled polymerization of functional monomers can be restricted as a result of steric constraints and coordination/reaction of the monomer with the catalyst, initiator or propagating chains.[22] To avoid this, protected monomers are often employed and deprotected postpolymerization to afford the desired functional polymers.[21,23,24] In addition, monomers with bulky pendent groups can suffer from poor conversion as a result of polymerization−depolymerization equilibrium.[25] Therefore, a facile and efficient route which provides access to a diverse range of highly corona-functionalized CCS polymers from a single scaffold would be immensely invaluable.

Recently, we reported the synthesis of a CCS polymer with high loadings of corona-isolated terminal alkyne (click) functionalities.[26] As a result of the efficient nature and functional group tolerance of CuAAC chemistry,[27−29] azido-substituted compounds with a range of functionalities can be grafted onto the alkyne CCS polymer scaffold to yield a wide variety of corona-functionalized star polymers from a single precursor. Herein we report the preparation of a clickable CCS polymer scaffold via an improved synthetic approach and study the grafting of various azido substituted compounds via CuAAC chemistry to afford highly corona-functionalized star polymers with unique and interesting architectures and properties. The grafting efficiency with different azido compounds and polymers was determined and factors affecting the click efficiency were investigated. Thus, this report provides a valuable reference for the high density functionalization of 3D nanostructures.

## EXPERIMENTAL SECTION

**Materials.** Anisole (anhydrous, 99.7%), 1-(chloromethyl)naphthalene (90%), copper(I) bromide (CuBr, 98%), copper(II) bromide ($CuBr_2$, 98%), methyl 2-bromopropionate (98%) chlorotrimethylsilane (98%), methacryloyl chloride (97%), 2-propyn-1-ol (99%), $\gamma$-oxo-1-pyrene butyric acid (tech.), 1,8-diazabicyclo[5.4.0]undec-7-ene (DBU, 98%), tetra-*n*-butyl ammonium fluoride (TBAF, 1 M solution in THF), stannous 2-ethylhexanoate ($Sn(Oct)_2$, 95%), stannous triflate ($Sn(OTf)_2$, 97%), $\beta$-cyclodextrin (98%), furfuryl isocyanate (97%), 1-bromodecane (98%), *N*,*N*,*N*′,*N*″,*N*″-pentamethyldiethylenetriamine (PMDETA, 99%), poly(ethylene glycol) monomethyl ether ($M_n$ ∼1000 Da), poly(ethylene glycol) monomethyl ether ($M_n$ ∼2000 Da), tetra-*n*-butylammonium hydrogen sulfate (TBAHS) (99+%), acetobromo-α-D-galactose (>93%), 4-(dimethylamino)pyridine (DMAP) (99%), sodium iodide (NaI, 99.999%), and potassium iodide (KI, ≥ 99.99%) were all purchased from Aldrich and used as received. Acetic acid (99.8%, Merck), *N*-(3-(dimethylamino)propyl)-*N*′-ethylcarbodiimide hydrochloride (EDCI) (98+%, Fluka), *N*,*N*-dimethylformamide (99.8%, Merck), *n*-hexane (AR, Chem-Supply), ethyl acetate (AR, Chem-Supply), methanol (MeOH, AR, Chem-Supply), thionyl chloride (Merck), sodium azide ($NaN_3$, 99%, Chem-Supply), silver chloride (AgCl, 99.5%, Fluka), poly(ethylene glycol) monomethyl ether ($M_n$ ∼350 Da) (Fluka), 9-anthracenecarboxylic acid (purum, Fluka), 1,8,9-anthrancenetriol (DIT, puriss, Fluka) and *trans*-2-[3-(4-*tert*.-butylphenyl)-2-methyl-2-propenylidene]-malononitrile (DCTB, puriss, Fluka) were also used as received. Tetrahydrofuran (RCI Labscan, HPLC) (THF) was distilled from sodium benzophenone ketyl. Toluene (Scharlau, HPLC), ε-caprolactone (CL, 99+%, Aldrich), dichloromethane (99.8%, Merck), triethylamine (99%, Ajax) and *tert*-butyl acrylate (98%, Aldrich) were distilled from calcium hydride (95%, Sigma-Aldrich). 2-Hydroxylethyl-2′-methyl-2′-bromopropionate **1** and 4,4′-bioxepanyl-7,7′-dione (BOD) were synthesized according to literature procedures.[30,31]

**Instrumentation.** Gel permeation chromatography (GPC) (THF as eluent) was performed on a Shimadzu liquid chromatography system fitted with a Wyatt DAWN EOS multiangle laser light scattering (MALLS) detector (690 nm, 30 mW) and a Wyatt OPTILAB DSP interferometric refractometer (690 nm), using three Phenomenex Phenogel columns (500, $10^4$, and $10^6$ Å porosity; 5 $\mu$m bead size) operated at 1 mL/min with column temperature set at 30 °C. GPC (DMF as eluent) was performed on a Shimadzu liquid chromatography system fitted with a Wyatt DAWN-HELEOS LS detector ($\lambda$ = 658 nm), Shimadzu RID-10 refractometer ($\lambda$ = 633 nm) and Shimadzu SPD-20A UV−vis detector, using three identical Polymer Laboratories PLgel columns (5 $\mu$m, MIXED-C) and HPLC grade DMF with 0.05 M LiBr (70 °C, 1 mL/min) as mobile phase. Astra software (Wyatt Technology Corp.) was used to process the data to determine the molecular weights either using known d*n*/d*c* values or based on the assumption of 100% mass recovery of the polymer where the d*n*/d*c* value was unknown. $^1$H NMR spectroscopic analysis was performed on a Varian Unity Plus 400 MHz spectrometer using the deuterated solvent as reference. Gas chromatography was performed on a Shimadzu GC 17-A gas chromatograph equipped with an Agilent J+W DB-5 capillary column (30 m, 5% phenyl siloxane) and coupled to a GCMS-QP50000 mass spectrometer (injector temperature =250 °C; initial column initial temperature =40 °C; heat ramp =10 °C/min; final column temperature =320 °C). Dynamic light scattering (DLS) measurements were performed using a Malvern high performance particle sizer (HPPS) with a 3.0 mW He−Ne laser operated at 633 nm. Analysis was performed at an angle of 173° and a constant temperature of 25 ± 0.1 °C. MALDI ToF MS was performed on a Bruker Autoflex III Mass Spectrometer operating in positive linear mode; the analyte, matrix (DIT or DCTB) and cationisation agent (NaI or KI) were dissolved in THF at concentrations of 10, 10, and 1 mg/mL, respectively, and then mixed in a ratio of 10:1:1. Then 0.3 $\mu$L of this solution was spotted onto a ground steel target plate, and the solvent was allowed to evaporate prior to analysis. FlexAnalysis (Bruker) was used to analyze the data. UV−vis spectrophotometry was performed on a Shimadzu UV-2101PC spectrometer using quartz cuvettes with a 1 cm path length.

**Synthesis of (Trimethylsilyl)propargyl Methacrylate (TMS-PgMA).** This compound was prepared according to the literature procedures.[31−33] $^1$H NMR (400 MHz, $CDCl_3$): $\delta_H$ 0.18 (*s*, 9H, $Si(CH_3)_3$), 1.96 (*m*, 3H, $CH_3$), 4.75 (*d*, 2H, $OCH_2$), 5.61 (*m*, 1H, CC*H*H *cis*), 6.17 (*m*, 1H, CCH*H* *trans*) ppm. $^{13}$C NMR (100 MHz, $CDCl_3$): $\delta_C$ −0.3 ($Si(CH_3)_3$), 18.3 ($CH_3$), 52.9 ($OCH_2$), 94.7 ($CH_2C{\equiv}C$), 99.1 ($CH_2C{\equiv}C$), 126.4 ($CCH_2$), 135.7 ($CCH_2$), 166.5 ($C{=}O$) ppm. LRMS [$M^+$]: $C_{10}H_{16}O_2Si$ requires 196.09; found, 196.10.

**Synthesis of HO-PCL-Br Macroinitiator 2.** A round-bottom flask charged with $Sn(Oct)_2$ (0.79 g, 1.95 mmol, 1 equiv) was evacuated and backfilled with argon. Subsequently, CL (20.0 g, 200 mmol, 100 equiv), 2-hydroxylethyl 2′-methyl-2′-bromopropionate **1** (0.823 g, 3.90 mmol, 2 equiv) and toluene (180 mL) were added via syringe. The reaction solution was stirred at 100 °C under argon for 19 h, cooled to room temperature and then precipitated into cold MeOH (800 mL). The precipitate was collected by vacuum filtration and dried *in vacuo* to yield macroinitiator **2** as a white powder, 19.0 g (91.2%). GPC-MALLS (THF): $M_n$ = 5.14 kDa, PDI = 1.20; $^1$H NMR (400 MHz, $CDCl_3$): $\delta_H$ 1.34−1.46 (*m*, $-CH_2CH_2CH_2-$), 1.61−1.72 (*m*, $-CH_2CH_2CH_2-$), 1.95 (*s*, $-CH_3$ end group), 2.32 (*t*, $-CH_2CH_2CO-$), 3.66 (*t*, $-CH_2CH_2OH$ end group), 4.07 (*t*, $-CH_2CH_2O-$) ppm. Different molecular weight macroinitiators were prepared by variation of the monomer to initiator ratio (Table S1, Supporting Information).

**Synthesis of HO-P(CL-*b*-TMS-PgMA)−Br Macroinitiator 3.** HO-PCL-Br macroinitiator **2** (3.00 g, 0.58 mmol, $M_{n,GPC}$ = 5.14 kDa, 1 equiv), TMS-PgMA (4.00 g, 20.4 mmol, 35 equiv), and PMDETA (0.20 g, 1.20 mmol, 2 equiv) were added to a Schlenk flask and dissolved

in anisole (19 mL). The mixture was subsequently degassed via one freeze−pump−thaw cycle, backfilled with argon and CuBr (85 mg, 0.58 mmol, 1 equiv) was added under argon. The mixture was then degassed via another two freeze−pump−thaw cycles, backfilled with argon and heated at 85 °C for 5 h. The reaction was stopped (TMS-PgMA conversion =50%) by dipping the reaction solution into liquid nitrogen. After warming to room temperature, the reaction solution was diluted with THF (100 mL) and passed through an alumina column to remove the copper complex. The solution was then concentrated to ∼15 mL in volume and precipitated into cold methanol (200 mL). The precipitate was collected by vacuum filtration and dried *in vacuo* to afford macroinitiator **3** as a white solid, 3.2 g (64%). GPC-MALLS (THF): $M_n$ = 8.66 kDa, PDI = 1.19. $^1$H NMR (400 MHz, $CDCl_3$): $\delta_H$ 0.17 (*s*, −Si($CH_3$)$_3$), 0.80−1.15 (*m*, −$CH_3$), 1.34−1.46 (*m*, −$CH_2CH_2CH_2$−), 1.61−1.72 (*m*, −$CH_2CH_2CH_2$−), 1.75−2.10 (*m*, −$CH_2$C− and *s*, −$CH_3$ end group), 2.32 (*t*, −$CH_2CH_2$CO−), 3.66 (*t*, −$CH_2CH_2$OH end group), 4.07 (*t*, −$CH_2CH_2$O−), 4.32−4.42 (m, −$CH_2CH_2$O− end group), 4.57 (*s*, −COO$CH_2$−) ppm. Different molecular weight macroinitiators were prepared by variation of the monomer to macroinitiator ratio (Table S1, Supporting Information).

**Synthesis of Alkyne Functional Stars CCS 1 and CCS 2.** Macroinitiator **3** (2.00 g, 0.289 mmol; $M_{n,GPC}$ = 8.66 kDa), BOD (0.65 g, 2.89 mmol), and stannous triflate (Sn(OTf)$_2$) (24.6 mg, 0.61 mmol) were added to a flask, and purged with argon. 2:8 THF/toluene (20 mL) was added and the reaction mixture was heated at 65 °C under argon for 99 h (cross-linker conversion via GC = 99+ %). The reaction mixture was filtered, concentrated and then fractionally precipitated (**SI**) with MeOH to isolate star **CCS 1**, 1.44 g; $M_{n,GPC}$ = 300 kDa, PDI = 1.25). The fractionated star **CCS 1** (1.44 g, 2.16 mmol of alkyne-TMS groups) and acetic acid (0.15 mL, 2.70 mmol) were dissolved in THF (24 mL) under argon at 0 °C and a 0.2 M TBAF solution in THF (10.8 mL) was added dropwise. The reaction solution was stirred at 0 °C for another 30 min and then at room temperature for a further 12 h. The reaction mixture was then concentrated to ∼5 mL in volume and precipitated into MeOH (50 mL). The precipitate was dried *in vacuo* to afford the terminal alkyne star **CCS 2**, 1.11 g (49%). GPC-MALLS (THF): $M_n$ = 267 kDa, PDI = 1.30. $^1$H NMR (400 MHz, $CDCl_3$): $\delta_H$ 0.80−1.20 (*m*, 3H, −$CH_3$), 1.35−1.47 (*m*, −$CH_2CH_2$CO−), 1.61−1.72 (*m*, −$CH_2CH_2CH_2$−), 1.80−2.10 (*m*, −$CH_2$C−), 2.32 (*t*, −$CH_2CH_2$CO−), 2.53 (*s*, C≡$CH$), 4.08 (*t*, −$CH_2CH_2$O−), 4.57 (*s*, −COO$CH_2$−) ppm (Figure S1, Supporting Information).

**Synthesis of Deprotected Arm Initiator HO-P(CL-*b*-PgMA)-Br (LP 1).** HO-P(CL-*b*-TMS-PgMA)-Br macroinitiator (Table S1, Supporting Information, entry 6) (0.50 g, 1.19 mmol of alkyne−TMS groups, $M_n$ = 11.3 kDa), and acetic acid (0.10 mL, 1.79 mmol) were dissolved in THF (12.8 mL) under argon at 0 °C and a 0.2 M TBAF solution in THF (5.8 mL) was added dropwise. The reaction solution was stirred at 0 °C for another 30 min and then at room temperature for a further 12 h. The reaction mixture was then concentrated to ∼5 mL in volume and precipitated into MeOH (20 mL). The precipitate was dried *in vacuo* to afford **LP 1**, 0.38 g (92%). GPC-MALLS (THF): $M_n$ = 9.2 kDa, PDI = 1.20. $^1$H NMR (400 MHz, $CDCl_3$): $\delta_H$ 0.80−1.20 (*m*, 3H, −$CH_3$), 1.35−1.47 (*m*, −$CH_2CH_2$CO−), 1.61−1.72 (*m*, −$CH_2CH_2CH_2$−), 1.80−2.10 (*m*, −$CH_2$C−), 2.32 (*t*, −$CH_2CH_2$CO−), 2.53 (*s*, C≡$CH$), 3.64 (*t*, −$CH_2CH_2$OH end group), 4.08 (*t*, −$CH_2CH_2$O−), 4.57 (*s*, −COO$CH_2$−) ppm.

**Synthesis of 3-Azidopropanol.** $NaN_3$ (2.80 g, 43.1 mmol) and TBAHS (85.0 mg, 0.25 mmol) were dissolved in Milli-Q water (50 mL). 3-Chloropropanol (2.04 g, 21.6 mmol) was then added and the mixture was stirred at 80 °C for 24 h. The mixture was extracted with diethyl ether (75 mL × 3) and the organic extracts were combined, dried ($MgSO_4$), filtered and concentrated *in vacuo* to yield a clear liquid, 1.80 g (82%). $^1$H NMR (400 MHz, $CDCl_3$): $\delta_H$ 1.82 (*quin*, 2H, $J$ = 6.6 Hz, $CH_2$), 1.91 (*br s*, 1H, $CH_2OH$), 3.44 (*t*, 2H, $J$ = 6.6 Hz, $CH_2N_3$), 3.74 (*t*, 2H, $J$ = 6.6 Hz, $CH_2O$) ppm. $^{13}$C NMR (100 MHz, $CDCl_3$): $\delta_C$ 31.4 ($CH_2$), 48.4 ($CH_2N_3$), 59.6 ($OCH_2$) ppm. LRMS [M − H$^+$]: $C_3H_7N_3O$ requires 100.11; found, 100.30.

**Synthesis of 1-(Azidomethyl)naphthalene C1.** 1-(Chloromethyl)naphthalene (2.00 g, 11.3 mmol), $NaN_3$ (1.47 g, 22.6 mmol), and DMF (50 mL) were heated at 65 °C for 24 h. The reaction mixture was centrifuged to remove excess $NaN_3$ and then the solvent was removed *in vacuo*. The residue was dissolved in dichloromethane (50 mL) and then washed with distilled water (50 mL × 3). The organic extract was dried ($MgSO_4$), filtered and concentrated *in vacuo* to afford **C1** as a brown powder, 1.90 g (86%). $^1$H NMR (400 MHz, $CDCl_3$): $\delta_H$ 4.78 (*s*, 2H, $CH_2N_3$), 7.42−7.61 (*m*, 4H, 4Ar$H$), 7.86−7.92 (*m*, 2H, 2Ar$H$), 8.02−8.05 (*m*, 1H, 1Ar$H$) ppm. $^{13}$C NMR (100 MHz, $CDCl_3$): $\delta_C$ 52.9 ($CH_2N_3$), 123.5 (ArCH), 125.2 (ArCH), 125.2 (ArCH), 126.7 (ArCH), 127.2 (ArCH), 128.8 (ArCH), 129.4 (ArCH), 131.0 (ArCC), 131.3 (ArCC), 133.9 (ArCC) ppm. LRMS [M$^+$]: $C_{11}H_9N_3$ requires 183.08; found, 183.30.

**Synthesis of 3-Azidopropyl Anthrancene-9-carboxylate C2.** Anthrancene carboxylic acid (2.22 g, 10.0 mmol) and thionyl chloride ($SOCl_2$) (30 mL) were added to a dried flask under argon. The reaction mixture was refluxed under argon for 90 min and the excess $SOCl_2$ was removed *in vacuo*. The resulting residue was azeotroped with benzene (10 mL × 3), redissolved in anhydrous THF (40 mL) and cooled to 0 °C. Triethylamine (2.4 mL, 32.7 mmol) was added, followed by 3-azidopropanol (0.97 g, 9.0 mmol) in anhydrous THF (30 mL) dropwise. The reaction solution was stirred at 0 °C for 30 min, warmed to room temperature and stirred for 48 h, and then filtered and concentrated. The crude product was redissolved in dichloromethane (50 mL), washed with 2 M NaOH (50 mL × 2), 2 M HCl (50 mL × 2) and distilled water (50 mL), dried ($MgSO_4$), filtered, and concentrated *in vacuo* to afford **C2** as a light brown solid, 2.5 g (90%). $^1$H NMR (400 MHz, $CDCl_3$): $\delta_H$ 2.09 (*quin*, 2H, $J$ = 6.4 Hz, $CH_2$), 3.45 (*t*, 2H, $J$ = 5.2 Hz, $OCH_2$), 4.67 (*t*, 2H, $J$ = 5.2 Hz, $CH_2N_3$), 7.44−7.54 (*m*, 4H, 4Ar$H$), 7.99−8.01 (*m*, 4H, 4Ar$H$), 8.48 (*s*, 1H, Ar$H$) ppm. $^{13}$C NMR (100 MHz, $CDCl_3$): $\delta_C$ 8.3 ($CH_2$), 48.2 ($CH_2N_3$), 62.5 ($OCH_2$), 124.7 (2ArCH), 125.6 (2ArCH), 127.2 (2ArCH), 127.7 (ArCH), 128.5 (ArCC), 128.7 (2ArCH), 129.5 (2ArCH), 131.0 (ArCH), 169.6 ($C$=O) ppm.

**Synthesis of 3-Azidopropyl 4-Oxo-4-(pyren-4-yl) Butanoate C3.** $\gamma$-Oxo-1-pyrenebutyric acid (1.20 g, 3.97 mmol), EDCI (0.840 g, 4.37 mmol), and DMAP (97.0 mg, 0.79 mmol) were dissolved in anhydrous dichloromethane (24 mL) under argon. 3-Azidopropanol (0.39 mL, 3.90 mmol) was then added and the mixture was stirred at 30 °C for 40 h. The reaction mixture was then washed with 0.05 M HCl (100 mL × 3), dried ($MgSO_4$), filtered and the filtrate concentrated *in vacuo*. The crude product was purified via column chromatography on silica using 2:8 hexane:dichloromethane. The desired compound ($R_f$ = 0.06) was collected, dried ($MgSO_4$), filtered and concentrated *in vacuo* (0.1 mbar, 50 °C) to give **C3** as a dark brown solid, 0.90 g (64%). $^1$H NMR (400 MHz, $CDCl_3$): $\delta_H$ 1.92 (*quin*, 2H, $J$ = 6.4 Hz, $CH_2$), 2.90 (*t*, 2H, $J$ = 6.4 Hz, $CH_2CO_2$), 3.39 (*t*, 2H, $J$ = 6.4 Hz, $CH_2N_3$), 3.53 (*t*, 2H, $J$ = 6.4 Hz, $COCH_2$), 4.23 (*t*, 2H, $J$ = 6.4 Hz, $CO_2CH_2$), 8.00−8.05 (*m*, 2H, 2Ar$H$), 8.13−8.23 (*m*, 5H, 5Ar$H$), 8.38 (*d*, 1H, $J$ = 8.0 Hz, Ar$H$), 8.91 (*d*, 1H, $J$ = 9.6 Hz, Ar$H$) ppm. $^{13}$C NMR (100 MHz, $CDCl_3$): $\delta_C$ 28.3 ($CH_2CO_2$), 28.9 ($CH_2$), 37.0 ($OCH_2$), 48.3 ($CH_2N_3$), 61.7 ($CO_2CH_2$), 124.1 (ArCH), 124.3 (ArCC), 124.8 (ArCC), 125.0 (ArCH), 126.1 (ArCC), 126.3 (ArCH), 126.3 (ArCH), 126.4 (ArCH), 127.1 (ArCH), 129.5 (ArCH), 129.6 (ArCC), 129.7 (ArCH), 130.5 (ArCH), 131.1 (ArCC), 131.7 (ArCC), 133.9 (ArCC) ppm.

**Synthesis of 3-Azidopropyl Furan-2-ylmethylcarbamate C4.** Furfuryl isocyanate (370 mg, 3.00 mmol) was dissolved in anhydrous THF (5 mL) in a dried Schlenk tube under argon, and 3-azidopropanol (300 mg, 2.97 mmol) and triethylamine (21 $\mu$L, 0.14 mmol) were added. After 24 h at 50 °C, the reaction mixture was concentrated

*in vacuo*, and purified via column chromatography on silica ($R_f$ = 0.73, 1:99 methanol:dichloromethane) to afford **C4** as a pale yellow oil, 420 mg (62%). $^1$H NMR (400 MHz, $CDCl_3$): $\delta_H$ 1.88 (*quin*, 2H, *J* = 8.0 Hz, $CH_2$), 2.29 (*t*, 2H, *J* = 8.0 Hz, $CH_2N_3$), 4.16 (*t*, 2H, *J* = 8.0 Hz, $OCH_2$), 4.34 (*d*, 2H, $CH_2N$), 5.05 (*br s*, N*H*), 6.21 (*d*, 1H, Ar*H*), 6.30 (m, 1H, Ar*H*), 7.34 (*m*, 1H, Ar*H*) ppm. $^{13}$C NMR (100 MHz, $CDCl_3$): $\delta_C$ 28.5 ($CH_2$), 38.9 ($CH_2N$), 48.2 ($CH_2N_3$), 62.0 ($OCH_2$), 107.2 (Ar*C*H), 110.4 (Ar*C*H), 142.2 (Ar*C*H), 151.5 (Ar*C*C), 156.0 (*C*=O) ppm. LRMS [$M^+$]: $C_9H_{12}N_4O_3$ requires 224.09; found, 224.00.

**Synthesis of β-Galactopyranosyl Azide C5.** β-Galactopyranosyl azide was prepared according to literature[34] with slight modification. To acetobromo-α-D-galactose (5.0 g, 12.2 mmol) in dichloromethane (50 mL) was added $NaN_3$ (4.40 g, 67.7 mmol), TBAHS (4.10 g, 12.2 mmol), and saturated $NaHCO_3$ (50 mL) in sequence. The reaction mixture was stirred vigorously at room temperature for 3 h and then diluted with ethyl acetate (500 mL). The organic layer was washed with saturated $NaHCO_3$ (200 mL) and concentrated *in vacuo*. The residue was dissolved in MeOH (35 mL) and a solution of 10 M KOH (9.0 mL) was added and stirred at room temperature for 3 h. The mixture was concentrated *in vacuo* and purified via column chromatography on silica using 3:7 MeOH/dichloromethane to afford **C5** as a white powder, 2.00 g (80%). $^1$H NMR (400 MHz, DMSO-$d_6$): $\delta_H$ 3.26−3.36 (*m*, 3H, 2C*H*OH, *H*-2,4, $CH_2CH$, *H*-5), 3.42−3.52 (*m*, 2H, $CH_2$OH, *H*-6), 3.63 (*d*, 1H, *CH*OH, *H*-3), 4.31 (*d*, 1H, *CH*$N_3$, *H*-1), 4.50−5.50 (*m*, 4H, 4O*H*, O*H*-2,3,4,6) ppm. $^{13}$C NMR (400 MHz, DMSO-$d_6$): $\delta_C$ 60.8 ($CH_2$, *C*-6), 68.5 (*CH*, *C*-2), 70.7 (*CH*, *C*-4), 73.7 (*CH*, *C*-3), 78.0 (*CH*, *C*-1), 91.1 (*CH*, *C*-5) ppm.

**Synthesis of Mono-6-deoxy-6-azido-β-cyclodextrin C6.** β-CD derivative **C6** was prepared according to a literature procedure.[35−38] β-Cyclodextrin (6.0 g, 5.29 mmol) was suspended in water (50 mL) and 8.25 M NaOH (2 mL) was added dropwise over 10 min. *p*-Toluenesulfonyl chloride (1.1 g, 5.67 mmol) in acetonitrile (30 mL) was added dropwise, causing immediate formation of a white precipitate. After 2 h at room temperature the precipitate was filtered off, redissolved in anhydrous DMF (20 mL) and $NaN_3$ (0.80 g, 12.3 mmol) was added. After 24 h at 65 °C the reaction solution was concentrated *in vacuo*, and the unwanted salts were removed via dialysis (Thermoscientific, MWCO 1000) against water for 48 h. The resultant aqueous suspension was collected and freeze-dried to afford a white solid, 0.6 g (10%). $^1$H NMR (400 MHz, DMSO-$d_6$): $\delta_H$ 3.26−3.80 (*br s*, 42H, 28C*H*O and 7$CH_2$O), 4.44−4.55 (*m*, 6H, 6O*H*), 4.80−4.90 (*m*, 7H, 7C*H*$O_2$), 5.60−5.80 (*m*, 14H, 14O*H*) ppm. $^{13}$C NMR (100 MHz, DMSO-$d_6$): $\delta_C$ 51.0 ($CH_2N_3$), 59.7−60.0 (*m*, $CH_2$O), 70.0−72.9 (*m*, *CH*O), 81.4−82.8 (*m*, *CH*O), 101.4−102.1 (*m*, *CH*$O_2$) ppm. MALDI ToF MS [$M + Na^+$]: $C_{42}H_{69}N_3NaO_{34}$ requires 1182.37; found, 1182.20.

**Synthesis of 1-Azidodecane C7.** 1-Bromodecane (5.03 g, 22.6 mmol) and $NaN_3$ (3.00 g, 46.1 mmol) were dissolved in DMF (50 mL) and heated at 65 °C for 24 h. After cooling to room temperature the reaction mixture was centrifuged to remove excess $NaN_3$ and washed with hexane (50 mL × 3). The hexane extracts were collected, dried ($MgSO_4$), filtered, and concentrated *in vacuo* to afford **C7** as a pale yellow oil, 4.0 g (97%). $^1$H NMR (400 MHz, $CDCl_3$): $\delta_H$ 0.87 (*t*, 3H, *J* = 6.8 Hz, $CH_3$), 1.25 (*m*, $CH_2$), 1.58 (*quin*, 2H, *J* = 6.8 Hz, $CH_2CH_2N_3$), 3.23 (*t*, 2H, *J* = 6.8 Hz, $CH_2N_3$) ppm. $^{13}$C NMR (100 MHz, $CDCl_3$): $\delta_C$ 14.2 ($CH_3$), 22.8 ($CH_2$), 22.9 ($CH_2$), 26.9 ($CH_2$), 29.0 ($CH_2$), 29.3 ($CH_2$), 29.5 ($CH_2$), 29.7 ($CH_2$), 29.7 ($CH_2$), 51.6 ($CH_2N_3$) ppm. LRMS [$M^+$]: $C_{10}H_{21}N_3$ requires 183.17; found, 182.50.

**Synthesis of Terminal Azido-Functionalized PEGs P1−3.** The general procedure employed for the preparation of terminal azido functionalized PEG was as follows: PEG monomethyl ether (20 mmol, 1 equiv) was initially dried via azeotropic distillation with toluene (100 mL × 3). Subsequently, triethylamine (24 mmol, 1.2 equiv) and dichloromethane (80 mL) were added and the mixture was cooled to 0 °C before methanesulfonyl chloride (30 mmol, 1.5 equiv) was added dropwise. The reaction was kept at 0 °C for 30 min and then at room temperature for 12 h. The reaction was filtered and the filtrate was concentrated *in vacuo*. The residue was dissolved in DMF (50 mL), and $NaN_3$ (200 mmol, 10 equiv) was added. The reaction mixture was heated to 65 °C for 12 h, cooled to room temperature and concentrated *in vacuo*. The residue was dissolved in water (200 mL) and then washed with dichloromethane (100 mL × 2). The organic extracts were collected, washed with water (200 mL) and saturated NaCl (200 mL × 2), dried ($MgSO_4$), filtered, and concentrated *in vacuo* to afford the desired monoazido PEGs. $^1$H NMR (400 MHz, $CDCl_3$): $\delta_H$ 3.37−3.41 (*s*, 3H, $OCH_3$ end group, and *t*, 2H, $CH_2N_3$ end group), 3.45−3.85 (*m*, −$CH_2$O−) ppm. MALDI ToF MS: **P1**, $M_n$ = 440, PDI = 1.01; **P2**, $M_n$ = 1070, PDI = 1.02; **P3**, $M_n$ = 1800, PDI = 1.02 (Figure S2−S4, Supporting Information).

**Synthesis of Terminal Azido-Functionalized PtBA P4.** The procedure to synthesize PtBA-$N_3$ was adopted from the literature[39] with slight modification. Deoxygenated acetone (4.2 mL) and *t*BA (15 g, 117 mmol) were added to a Schlenk tube. The solution was degassed by three freeze−pump−thaw cycles and then CuBr (170 mg, 1.17 mmol), $CuBr_2$ (14 mg, 0.63 mmol) and PMDETA (250 μL, 1.18 mmol) were added. The reaction solution was stirred at room temperature for 30 min and then methyl 2-bromopropionate (270 μL, 2.34 mmol) was added under argon. The reaction mixture was heated at 65 °C for 13 h (monomer conversion via GC = 50%), cooled to room temperature and precipitated into cold methanol (−15 °C, 600 mL). The precipitate was collected and redissolved in DMF (50 mL). $NaN_3$ (1.52 g, 23.4 mmol) was added and the reaction mixture was then stirred at room temperature for 24 h. The solvent was removed *in vacuo* and the residue was redissolved in dichloromethane (50 mL) and washed with saturated NaCl (50 mL × 2) and distilled water (50 mL × 2). The organic extract was collected, dried ($MgSO_4$), filtered and concentrated *in vacuo* to afford PtBA-$N_3$ **P4**, 6.00 g (38.5%); GPC-MALLS: $M_n$ = 5.85 kDa, PDI = 1.12. $^1$H NMR (400 MHz, $CDCl_3$): $\delta_H$ 1.14 (*s*, 3H, −C($CH_3$)−), 1.20−2.00 (*m*, −C($CH_3$)$_3$, and −$CH_2$CH−), 2.00−2.50 (*m*, −$CH_2CH$−), 2.90−3.00 (*d*, −$CH_2N_3$ end group), 3.66 (s, −$OCH_3$ end group) ppm. MALDI ToF MS: $M_n$ = 3.60 kDa, PDI = 1.08. (Figure S5, Supporting Information).

**Synthesis of Highly Functionalized CCS Polymers via CuAAC Chemistry.** The general procedure for synthesizing corona-functionalized stars **CCS C1-5**, **CCS C7**, and **CCS P4** was as follows: initially a 0.085 mM catalyst stock solution was prepared by dissolving CuBr (0.085 mmol, 1 equiv), and PMDETA (0.085 mmol, 1 equiv) in degassed DMF. In a Schlenk tube, alkyne star **CCS 2** (0.187 μmol, 0.084 mmol alkyne groups, 1 equiv) and the azido compound (0.42 mmol, 5 equiv or 0.17 mmol, 2 equiv **P4** only) were dissolved in DMF (5 mL). The mixture was degassed via two freeze−pump−thaw cycles and backfilled with argon, and catalyst stock solution (0.1 mL) was added. The reaction solution was subjected to one freeze−pump−thaw cycle, backfilled with argon and stirred at room temperature for 48 h. The Cu(I) catalyst was removed via addition of 1-dodecanethiol (0.088 mmol, 1 equiv) to form an insoluble copper complex (the solution immediately became cloudy and the characteristic color of the CuBr/PMDETA complex completely disappeared). After a further 24 h at room temperature the reaction mixture was centrifuged to remove the insoluble copper salts, and the supernatant was concentrated *in vacuo* to ∼1−2 mL in volume and then precipitated in methanol (25 mL) twice. The precipitate was collected via centrifugation and dried *in vacuo* to give the click-functionalized stars.

The general procedure for synthesizing corona-functionalized stars **CCS P1−3** and **CCS C6** was as follows: initially a 0.085 mM catalyst stock solution was prepared by dissolving CuBr (0.085 mmol, 1 equiv), and PMDETA (0.085 mmol, 1 equiv) in degassed DMF. In a Schlenk tube, alkyne star **CCS 2** (0.187 μmol, 0.084 mmol of alkyne groups, 1 equiv) and the azido compound (0.17 mmol, 2 equiv) were dissolved

in DMF (5 mL). The mixture was degassed via two freeze−pump−thaw cycles and backfilled with argon, and catalyst stock solution (0.1 mL) was added under argon. The reaction solution was subjected to one freeze−pump−thaw cycle, backfilled with argon, and stirred at room temperature for 48 h. The Cu(I) catalyst was removed via addition of 1-dodecanethiol (0.088 mmol, 1 equiv) to form an insoluble copper complex. After a further 24 h at room temperature, the reaction mixture was centrifuged to remove the insoluble copper salts. The supernatant was dialyzed (Thermoscientific, MWCO = 3500) against water for 4 days and freeze-dried to afford the click-functionalized stars.

**Synthesis of Highly Functionalized Linear Polymers via CuAAC Chemistry.** The general procedure for synthesizing linear polymers (**LP C2**, **LP C6**, and **LP P2**) with high pendent functionality was as follows: initially a 150 mM catalyst stock solution was prepared by dissolving CuBr (150 mmol, 1 equiv) and PMDETA (150 mmol, 1 equiv) in degassed DMF. In a Schlenk tube, deprotected macroinitiator **LP 1** (5.43 $\mu$mol, 0.147 mmol alkyne groups, 1 equiv) and the azido compound (0.29 mmol, 2 equiv or 0.74 mmol, 5 equiv **C2** only) were dissolved in DMF (4 mL). The mixture was degassed via two freeze−pump−thaw cycles, backfilled with argon and catalyst stock solution (0.1 mL) was added. The reaction solution was subjected to one freeze−pump−thaw cycle, backfilled with argon and stirred at room temperature for 48 h. The Cu(I) catalyst was removed via addition of 1-dodecanethiol (0.150 mmol, 1 equiv) to form an insoluble copper complex (the solution immediately became cloudy and the characteristic color of the CuBr/PMDETA complex completely disappeared). After a further 24 h at room temperature the reaction mixture was centrifuged to remove the insoluble copper salts. For the synthesis of **LP C6** and **LP P2**, the supernatant was dialyzed (Thermoscientific, MWCO = 3500) against water for 4 days and freeze-dried to afford the grafted linear polymer. For **LP C2**, the supernatant was concentrated *in vacuo* to ∼1−2 mL in volume and then precipitated in methanol (25 mL) twice. The precipitate was collected via centrifugation and dried *in vacuo* to give the grafted linear polymer. GPC-MALLS (THF): **LP C2** $M_n$ = 43.4 kDa, PDI = 1.52. GPC-MALLS (DMF): **LP C6** $M_n$ = 26.7 kDa, PDI = 1.15; **LP P2** $M_n$ = 39.7 kDa, PDI = 1.27.

## RESULTS AND DISCUSSION

**Improved Synthesis of "Clickable" CCS Polymer Scaffold.** In our previous publication two issues were encountered during the preparation of alkyne CCS polymers, including poor macroinitiator-to-star conversion and star−star coupling.[26] Therefore, a new synthetic strategy was developed to overcome these problems. Initially, the alkyne CCS polymer scaffold was prepared via the arm-first approach to act as a versatile platform for the preparation of a diverse library of highly functionalized stars with tunable structures and properties (Scheme 1). In the arm formation step, macroinitiator **3** was first synthesized via ROP of $\varepsilon$-caprolactone (CL) and subsequent atom transfer radical polymerization (ATRP) of trimethylsilyl propargyl methacrylate (TMS-PgMA) using the asymmetric difunctional initiator 2-hydroxyethyl 2′-methyl-2′-bromopropionate **1** (Scheme 1, routes (i) and (ii), respectively). In the star formation step (Scheme 1, route (iii), ROP of 4,4′-bioxepanyl-7,7′-dione (BOD) cross-linker using macroinitiator **3** and $Sn(OTf)_2$ as catalyst yielded star **CCS 1** with TMS protected alkyne functionalities. The TMS protecting groups on the corona of **CCS 1** were removed using TBAF (Scheme 1, route (iv) to afford **CCS 2** with clickable terminal alkyne groups suitable for the subsequent CuAAC functionalization.

In the arm formation step, ROP and ATRP were repeated several times with various monomer to initiator ratios as to afford

**Scheme 1. Synthetic Routes for the Preparation of Highly Corona-Functionalized CCS Polymers via Sequential ROP, ATRP, and CuAAC Chemistry**[a]

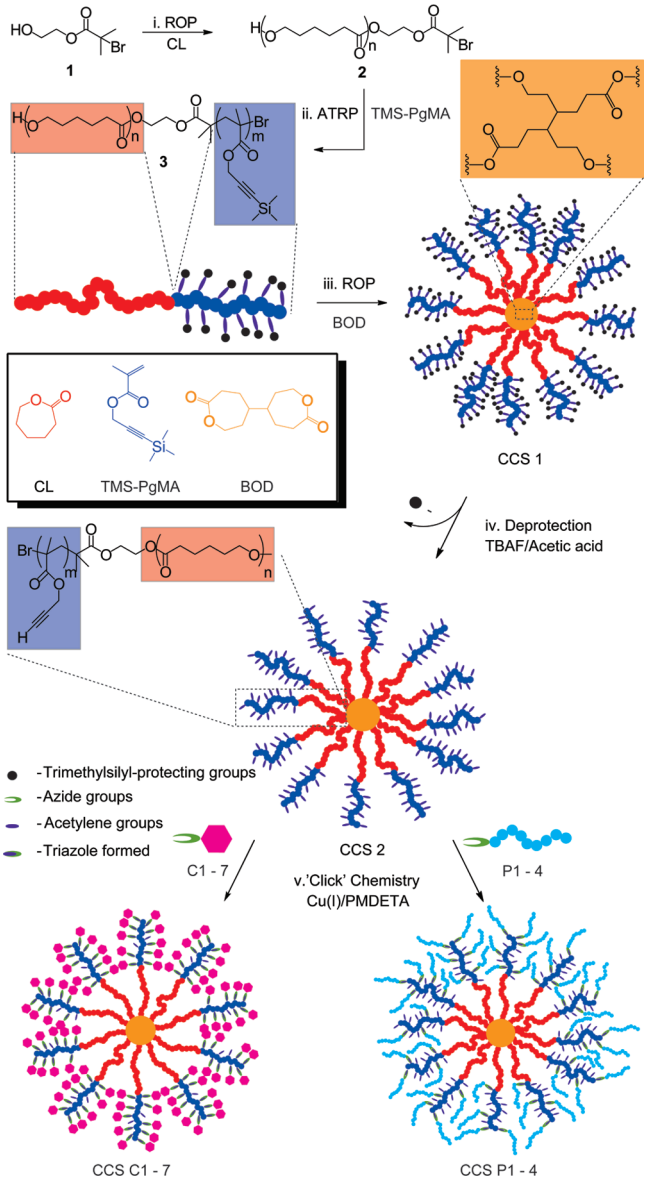


[a] Key: (i) formation of poly($\varepsilon$-caprolactone) macroinitiator (HO-PCL-Br) **2** through ROP of CL using initiator **1**; (ii) synthesis of poly($\varepsilon$-caprolactone-*b*-trimethylsilyl propargyl methacrylate) macroinitiator (HO-P(CL-*b*-TMS-PgMA)-Br) **3** through ATRP of TMS-PgMA using macroinitiator **2**; (iii) preparation of alkyne functionalized star **CCS 1** via the arm-first approach and ROP of BOD cross-linker with macroinitiator **3**; (iv) deprotection of TMS-protected **CCS 1** using TBAF in acetic acid to afford terminal alkyne functionalized star **CCS 2**; (v) corona functionalization of **CCS 2** via CuAAC chemistry using CuBr/PMDETA as the catalyst.

macroinitiators **2** and **3** with various degrees of polymerization; the theoretical and determined molecular weight characteristics and monomer unit ratios indicated good control of the polymerization was observed in all cases (Table S1, Supporting Information). A TMS protected PgMA monomer was employed to minimize potential side reactions, including propagating radical addition to terminal alkyne moieties (leading to branched

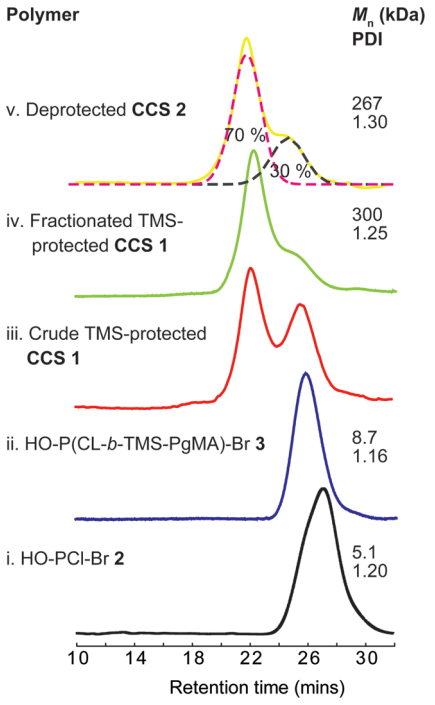


**Figure 1.** GPC (THF) refractive index (RI) chromatograms of (i) HO-PCL-Br macroinitiator **2** ([**1**]:[$Sn(Oct)_2$]:[CL] = 2:1:80, 110 °C in toluene) (Table S1, Supporting Information, entry 2); (ii) HO-P(CL-*b*-TMS-PgMA)-Br macroinitiator **3** ([**2**]:[CuBr]:[PMDETA]:[TMS-PgMA] = 1:1:2:35, 80 °C in anisole) (Table S1, Supporting Information, entry 4); (iii) crude **CCS 1** ([**3**]:[$Sn(OTf)_2$]:[BOD] = 10:1:100, 65 °C in 1:4 THF:Toluene); (iv) fractionated **CCS 1**; (v) deprotected **CCS 2** polymer consisting of 70% CCS polymer and 30% unincorporated polymer as determined by deconvolution of the RI chromatograms using Gaussian functions.

or cross-linked products at high monomer conversions[23,32]) and strong coordination of terminal alkynes to Cu(I) complexes (such as those commonly used as ATRP catalysts).[40,41] Polymers prepared from each synthetic step were characterized via GPC (Figure 1) and $^1$H NMR spectroscopic analysis (Figure S1, Supporting Information). The GPC results show a decrease in elution times corresponding to molecular weight increases across each synthetic stage. Low polydispersities (PDI < 1.30) were observed for all polymers prepared indicating narrow molecular weight distributions and controlled polymeric architectures were generated in all cases.

In the star-formation step, stannous triflate ($Sn(OTf)_2$) was used as the catalyst for ROP of the BOD cross-linker, allowing the alkyne star **CCS 1** to be prepared under milder reaction conditions at a temperature of 65 °C. In comparison to the previously reported synthesis using stannous 2-ethylhexanoate ($Sn(Oct)_2$) as the catalyst at 100 °C,[26] $Sn(OTf)_2$ provides significantly improved macroinitiator-to-star conversions from 40% to 60%, and reduced the amount of the star−star coupling from approximately 15% to <1% (Figure 1, curve (iii)). Overall, the new $Sn(OTf)_2$ catalytic system utilized increased the yield of the CCS polymers from 31% to 50% due to the elimination of high molecular weight star−star coupled products.[26] These results indicate that $Sn(OTf)_2$ and the lower reaction temperature suppresses transesterification during ROP,[42,43] minimizing intramolecular backbiting of terminal hydroxyl groups and intermolecular transesterification. Intramolecular backbiting leads to cyclization of the arm macroinitiators resulting in loss of their active hydroxyl terminus, thus preventing them from participating in ROP and integration into the CCS polymers. Intermolecular transesterification at high BOD conversions would result in active hydroxyl initiating sites in the core of preformed CCS polymers attacking ester moieties of adjacent CCS polymers, which is believed to be the major cause of star−star coupling. Lowering the reaction temperature would suppress both types of transesterification and allow high macroinitiator-to-star conversions with minimal star−star coupling. $Sn(OTf)_2$ has been reported[42,43] to be capable of catalyzing ROP of lactones at low temperatures and fast reaction rates. The results obtained in this study suggest $Sn(OTf)_2$ is a superior catalyst for the synthesis of alkyne functionalized CCS polymers. The crude CCS polymer was purified via fractional precipitation to afford the fractionated star **CCS 1** with a $M_n$ of 300 kDa and low PDI of 1.25 (Figure 1, curve (iv)). From the molecular weight and conversion data the average number of arms (*f*) incorporated into each CCS polymer was calculated to be 25 with each arm containing ∼18 pendent TMS protected alkyne groups; thus, each star possess ∼450 alkyne groups (**SI**). Even after multiple fractional precipitations, clean separation of **CCS 1** could not be achieved as evidenced from a shoulder at high retention time (Figure 1 (iv)), which corresponds to unincorporated polymer. Following the isolation of **CCS 1**, the alkyne groups on the corona were deprotected to afford alkyne star **CCS 2** (Scheme 1, route (iv)) with a $M_n$ of 267 kDa, which correlates well with the theoretical value of 265 kDa (Figure 1, curve (v)), based upon the $M_n$ of **CCS 1** and number of alkyne groups per star. GPC and $^1$H NMR spectroscopic analysis (Figure S1, Supporting Information) indicate that no degradation of the PCL components occurs under the acidic deprotection conditions. Deconvolution of the GPC RI chromatogram of **CCS 2** (Figure 1, curve (v) provided an estimate of 70% deprotected CCS polymer and 30% unincorporated polymer. The 30% unincorporated polymer is likely to originate from "arm" macroinitiator **3** that has been chain extended[1] with BOD but not incorporated into CCS polymers (i.e., P(BOD-*b*-CL-*b*-TMS-PgMA)). There are two possible causes for the presence of unconverted P(BOD-*b*-CL-*b*-TMS-PgMA): (i) during the ROP-mediated CCS formation some of the BOD chain extended macroinitiators P(BOD-*b*-CL-*b*-TMS-PgMA) are terminally inactive,[44,45] due to insufficient Sn(II) catalyst being available to complex with the hydroxyl group of the macroinitiator and initiate cross-linking, as the Sn(II) catalysts are mostly trapped in the core of the preformed CCS polymers, and (ii) the inactive macroinitiators with pendent cross-linkable functionality cannot diffuse effortlessly into the preformed CCS polymers and are therefore not incorporated due to steric restrictions;[1,44] thus, prolonged polymerization times would be required to convert all the unreacted macroinitiators. The unincorporated P(BOD-*b*-CL-*b*-TMS-PgMA) present in the crude CCS cannot be completely isolated via fractional precipitation (Figure 1 (iv)) and this most likely results in the 30% unincorporated polymer in the final alkyne CCS polymer product (Figure 1, curve (v)).

**Synthesis of Azido-Substituted Compounds.** Following the improved synthesis of the alkyne CCS polymer scaffold **CCS 2**, a range of azido substituted derivatives (Figure 2) were prepared to demonstrate the versatility of the click approach toward the preparation of a library of highly corona-functionalized stars and to assess factors affecting the 'click' efficiency.

The azido-substituted compounds prepared in this study can be divided into four main classes: (i) polycyclic aromatic hydrocarbons, including 1-(azidomethyl)-naphthalene **C1**, 3-azidopropyl

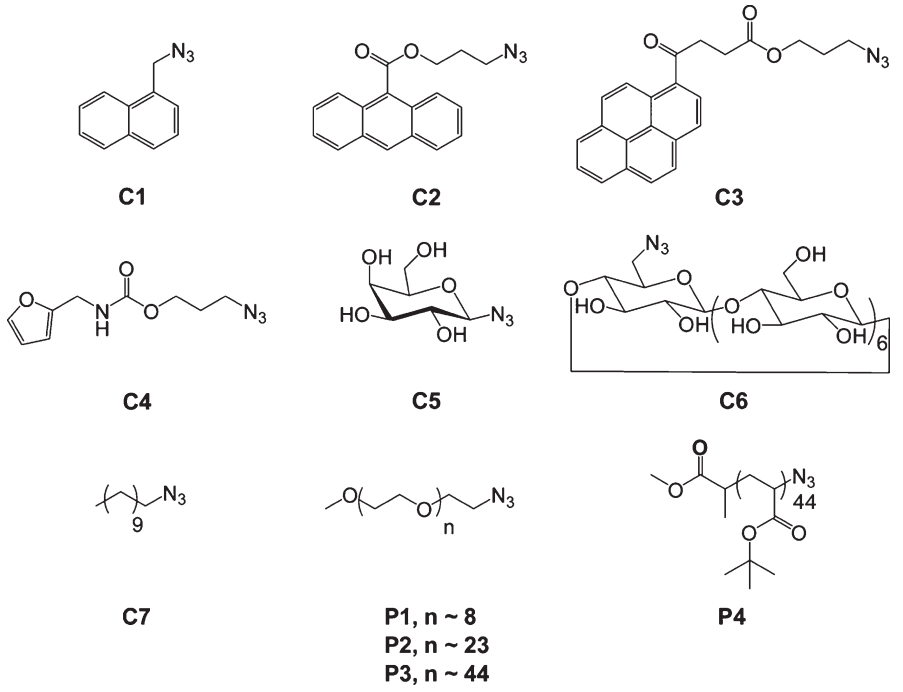


**Figure 2.** Structures of azido-substituted compounds **C1**−7 and terminal azido functionalized polymers **P1**−**4** employed for click functionalization of alkyne star **CCS 2**.

anthrancene-9-carboxylate **C2** and 3-azidopropyl 4-oxo-4-(pyren-4-yl) butanoate **C3**; (ii) saccharides, including $\beta$-galactopyranosyl azide **C5** and mono-6-deoxy-6-azido-$\beta$-cyclodextrin **C6**; (iii) small hydrophobic molecules with linear structures, including 3-azidopropyl furan-2-ylmethylcarbamate **C4** and 1-azidodecane **C7**, and; (iv) macromolecules, including PEG with various molecular weights (**P1**−3) and poly(*t*-butyl acrylate) (P*t*BA) **P4**. The successful synthesis of **C1**−**7** was confirmed by NMR spectroscopic analysis, GC-MS and MALDI ToF MS (**C6** only). Azido terminated PEG with various molecular weights ($M_n$ = 440, 1070, and 1800 kDa) were prepared by mesylation of poly(ethylene glycol) monomethyl ether followed by azide substitution and characterized via GPC, $^1$H NMR spectroscopic analysis and MALDI ToF MS. Quantification of the degree of azide substitution was achieved using $^1$H NMR spectroscopic analysis and MALDI ToF MS (Figures S2−S4, Supporting Information), which revealed a high degree of azide functionalization (>85%) for all PEG samples. Terminal azido P*t*BA **P4** was prepared first via ATRP of *tert*-butyl acrylate using methyl 2-bromopropionate as the initiator followed by substitution of the $\omega$-bromo group with azide. The polymer **P4** was analyzed via GPC, $^1$H NMR spectroscopic analysis and MALDI ToF MS, with the latter revealing quantitative azide substitution (Figure S5, Supporting Information) in agreement with the literature.[46]

**Functionalization of Alkyne CCS Polymer Scaffold via CuAAC.** Functionalization of the alkyne CCS polymer scaffold **CCS 2** was achieved by grafting the azido substituted compounds **C1**−7 and **P1**−**4** via CuAAC chemistry using Cu(I)/PMDETA as the catalyst (Scheme 1, route (v)) to afford **CCS C1**−7 and **CCS P1**−**4**, respectively (Table 1). The reactions were performed by adding an excess of the azido substituted compounds to a 0.037 mM (16.8 mM pendent alkyne groups) solution of **CCS 2**. This solution was subjected to several freeze−pump−thaw cycles prior to the addition of a degassed Cu(I)/PMDETA catalyst stock solution (20 mol % relative to alkyne) to prevent oxidation of the catalyst and possible side reactions. All reactions were conducted under argon at room temperature for 48 h. Low reaction temperatures and catalyst loadings were employed to suppress potential side reactions, and long reaction times were used to compensate for the retarded rate of CuAAC chemistry resulting from steric congestion of the pendent alkyne groups. At the end of the reactions, the Cu/PMDETA catalyst was isolated via the addition of excess dodecanthiol,[47] which forms an insoluble copper complex that can be removed by filtration. Incomplete removal of copper complex was found to lead to gel formation as the result of star−star coupling upon isolation of the functionalized stars (Scheme 2). All click-functionalized CCS polymers (except **CCS P4**) were isolated from the crude reaction solution via precipitation or dialysis and characterized by GPC, $^1$H NMR spectroscopic analysis and DLS (Table 1).

As a result of the unique architecture of the click-functionalized stars (Scheme 1), GPC systems (using THF or DMF as the mobile phase) equipped with MALLS detectors were employed to calculate the molecular weight characteristics of the CCS polymers based upon the assumption of 100% mass recovery,[48] since this allows the absolute molecular weights to be determined independent of the polymers' architectures. $^1$H NMR spectroscopic analysis was predominately used to quantify the grafting efficiency of azido substituted compounds, since GPC might give erroneous results due to possible intermolecular coupling of star polymers. Furthermore, dynamic light scattering (DLS) was employed to investigate the variation in hydrodynamic volume of the CCS polymers upon click-functionalization. The $M_n$ of the functionalized CCS polymers calculated via GPC (Table 1) revealed an increase from 267 (**CCS 2**) to 320−885 kDa depending on the clicked compound. DLS results revealed an increase of the hydrodynamic volumes of the functionalized

**Table 1. Characterization of Corona-Functionalized CCS Polymers**

| polymer | mass[a] (g mol$^{-1}$) | CE[b] (%) | error[c] ± (%) | functional units no.[d] | $M_n^{theo}$ (kDa) | $M_n^{NMR}$ (kDa)[e] | $M_n^{GPC}$ (kDa)[f] | PDI | $D_h$[g] (nm) |
|---|---|---|---|---|---|---|---|---|---|
| **CCS 1**[h] | - | - | - | - | - | - | 300 | 1.25 | 29.6 |
| **CCS 2** | - | - | - | - | 265 | - | 267/(257[i]) | 1.30 | 18.0(25.5[j]) |
| **CCS C1** | 183.2 | 99+ | 10 | 450 | 358 | 358 | 330 | 1.35 | 18.6 |
| **CCS C2** | 305.3 | 86 | 9 | 388 | 413 | 395 | 427 | 1.60 | 30.8 |
| **CCS C3** | 383.1 | 76 | 8 | 344 | 448 | 408 | 449 | 1.14 | 28.0 |
| **CCS C4** | 224.1 | 99 | 10 | 445 | 377 | 376 | 424 | 1.08 | 32.1 |
| **CCS C5** | 205.1 | 18 | 2 | 82 | 368 | 293 | 320[i] | 1.31 | 33.8[j] |
| **CCS C6** | 1160.0 | 43 | 4 | 192 | 798 | 499 | 520[i] | 1.29 | 31.6[j] |
| **CCS C7** | 183.3 | 99+ | 11 | 450 | 358 | 358 | 345 | 1.25 | 22.6 |
| **CCS P1** | 440[k] | 93 | 10 | 418 | 450 | 437 | 455[i] | 1.75 | 30.1 |
| **CCS P2** | 1070[k] | 64 | 7 | 286 | 726 | 562 | 618[i] | 1.54 | 70.2 |
| **CCS P3** | 1800[k] | 43 | 4 | 193 | 1176 | 662 | 885[i] | 1.56 | 145.8 |
| **CCS P4** | 6840[l] | 10 | - | 45 | - | - | - | - | - |

[a] Molecular weight for corresponding azido substituted compound. [b] Click efficiency determined by $^1$H NMR spectroscopic analysis. [c] Error of click efficiency calculation based upon $^1$H NMR spectroscopic analysis resonance integrations. [d] Number of azido substituted compounds attached per star. [e] Number average molecular weight of functionalized stars determined by $^1$H NMR spectroscopic analysis. [f] Number average molecular weight of functionalized stars determined by GPC (THF) and based upon the assumption of 100% mass recovery. [g] Hydrodynamic diameter of functionalized stars determined by DLS at 25 ± 0.1 °C. [h] Protected alkyne star polymer prepared using macroinitiator **3** (Table S1, Entry 4). [i] Molecular weight measurement determined by GPC (DMF) and based upon the assumption of 100% mass recovery.[48] [j] DLS measurement using DMF as solvent at 25 ± 0.1 °C. [k] Number average molecular weight calculated using MALDI ToF MS. [l] Number average molecular weight measured by GPC (THF) based upon the assumption of 100% mass recovery.

**Scheme 2. Side Reactions That Could Potentially Cause Star−Star Coupling During CuAAC Reactions, Including (a) Sonogashira-Type Coupling, (b) Radical dimerization, and (c) Glaser Coupling**

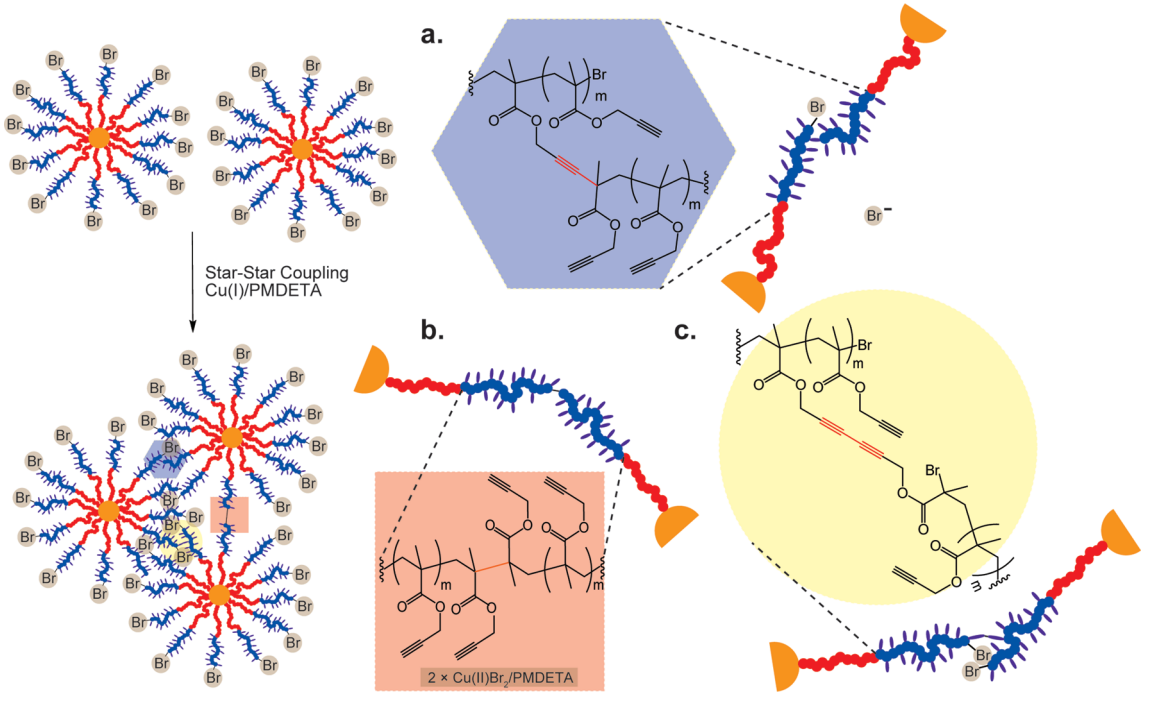


stars after click modification, with hydrodynamic diameters ($D_h$) increasing from 18 to 18.6−145.8 nm. From $^1$H NMR spectroscopic analysis the number of functional compounds attached to each CCS polymer ranged from 45 to 450 and was highly dependent on their structure and functionality. Interestingly, it was noted that some of the functionalized CCS polymers suffer from increased polydispersities (>1.30) and $M_n$ values calculated via GPC are generally higher than those determined by $^1$H NMR spectroscopic analysis, which indicates possible star−star coupling as a result of side reactions. Three possible side reactions that might lead to star−star coupling are illustrated in Scheme 2.


dx.doi.org/10.1021/ma200283c |*Macromolecules* 2011, 44, 3189–3202

(i) Sonogashira-type coupling of terminal α-carbon on CCS polymer arms with pendent alkyne groups along the arms of the other CCS polymer (after elimination of the terminal bromide groups) can be catalyzed by Cu(I) and tertiary bases (e.g., PMDETA) leading to the formation of star−star coupled products (Scheme 2a). (ii) In absence of oxygen (or other radical scavengers) Cu(I)/PMDETA abstracts bromine atoms from the CCS polymers to form terminal radical sites that can undergo intermolecular dimerization, resulting in star−star coupling (Scheme 2b). (iii) In the presence of oxygen or a base (e.g., PMDETA), Cu(I) can catalyze the Glaser coupling of terminal alkynes (Scheme 2c).[49] Thus, intermolecular coupling of pendent terminal alkynes on CCS polymers could lead to star−star coupling. Intermolecular couplings can not be detected using characterization techniques such as $^1$H NMR spectroscopic analysis since characteristic resonances resulting from side-reactions are insignificant compared to resonances from the polymer. It is evident that even small proportions of coupling reactions can lead to detrimental effects on the molecular weight characteristics of the functionalized star polymers, and given the high functional density of the corona the chance of coupling reactions is amplified.

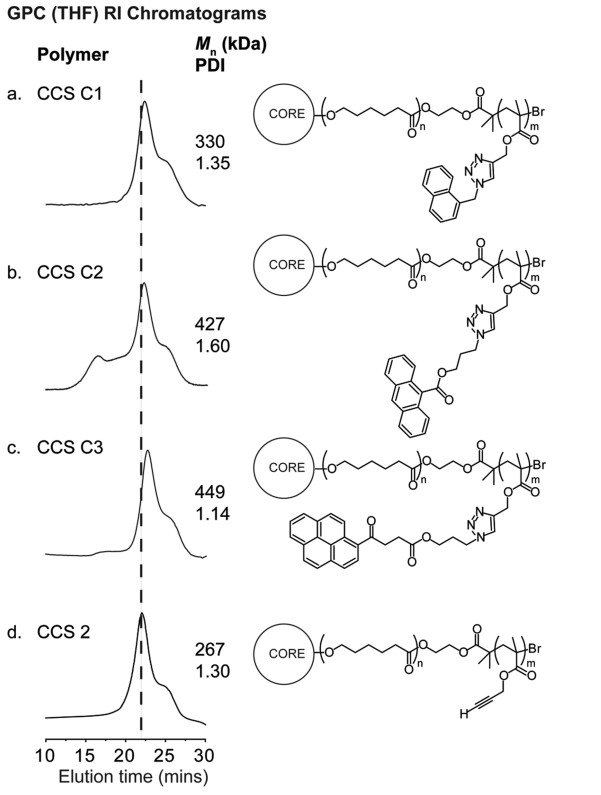


**Figure 3.** GPC (THF) RI chromatograms for (a) naphthalene, (b) anthracene and (c) pyrene corona-functionalized stars **CCS C1−3**, respectively, and (d) alkyne CCS polymer scaffold **CCS 2**.

**Synthesis of Fluorescent CCS Polymers.** Fluorescent stars **CCS C1−3** carrying a high number of polycyclic aromatic hydrocarbons were prepared through grafting of azido substituted naphthalene, anthracene and pyrene (**C1−3**, respectively) derivatives onto **CCS 2** via CuAAC chemistry. $^1$H NMR spectroscopic analysis (*vide infra*) revealed that the grafting was successful in all cases with the click efficiency decreasing as the number of aromatic units increased. For stars **CCS C1−3** GPC-MALLS provided increases in molecular weight (Table 1), although interestingly the RI chromatograms (Figure 3) revealed slight shifts to higher elution time. This unexpected shift may originate from an increase in structure rigidity of the functionalized stars causing delayed elution similar to that reported in linear polymer cyclization.[50] Furthermore, the high density of aromatic groups on the stars corona may interact with the column material (cross-linked polystyrene) through $\pi-\pi$ stacking, thus causing a delay in their elution.

Closer examination of the GPC RI chromatogram for the anthracene corona-functionalized star **CCS C2** revealed a bimodal distribution (Figure 3b) with broad polydispersity and higher than theoretically predicted $M_n$. These results indicate the occurrence of star−star coupling, which might result from the previously described click side-reactions, but more likely, anthracene dimerization in the presence of light.[51−53] As a result of the chromophoric nature of the polycyclic aromatic hydrocarbon derivatives used it was possible to quantify their loading via UV−vis spectroscopic analysis, as demonstrated for the pyrene corona-functionalized star **CCS C3** (Figure 4).

UV−vis spectra of pyrene derivative **C3** were recorded at known concentrations and the absorption measured at 354 nm to generate a calibration curve from which the excitation coefficient was determined to be 60000 $M^{-1}cm^{-1}$ (Figure 4). Utilizing this

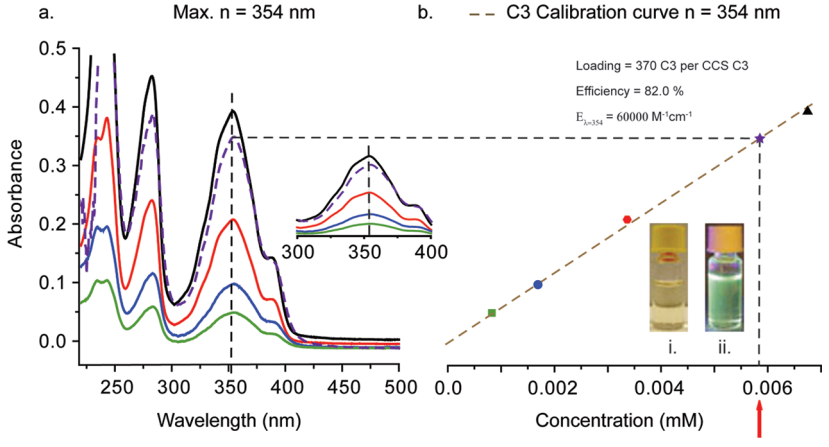


**Figure 4.** (a) UV−vis spectra (THF) for pyrene corona-functionalized star **CCS C3** and azido pyrene **C3**. (b) Calibration curve for **C3** and determination of **CCS C3** pyrene loading. Inset: THF solution of **CCS C3** under (i) white light and (ii) UV irradiation ($\lambda$ = 254 nm).


dx.doi.org/10.1021/ma200283c |*Macromolecules* 2011, 44, 3189–3202

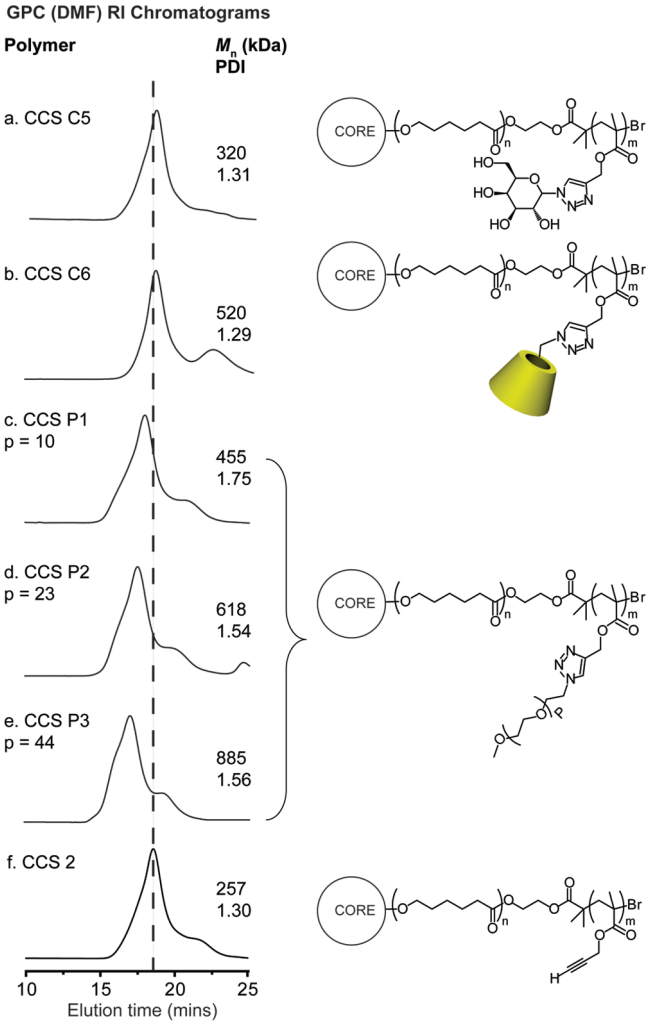


**Figure 5.** GPC (DMF) RI chromatograms of (a) $\beta$-galactose corona-functionalized star **CCS C5**, (b) $\beta$-CD corona-functionalized star **CCS C6**, (c) $PEG_{400}$, (d) $PEG_{1000}$ and (e) $PEG_{2000}$ corona-functionalized stars **CCS P1-3**, respectively, and (f) alkyne CCS polymer scaffold **CCS 2**.

excitation coefficient the loading of pyrene molecules at the corona of star **CCS C3** was calculated to be 370, which is similar to that determined via $^1$H NMR spectroscopic analysis (Table 1). Furthermore, the fluorescent nature of **CCS C3** was demonstrated upon UV irradiation ($\lambda$ = 254 nm) (Figure 4), which provides additional evidence for the successful incorporation of pyrene.

**Synthesis of Amphiphilic CCS Polymers.** Amphiphilic CCS polymers with hydrophobic polyester-based cores and inner shells, and hydrophilic coronas were prepared through grafting **CCS C2** with hydrophilic azido substituted saccharides **C5** and **C6**, and PEGs **P1**−**3**; GPC RI chromatograms for the resulting amphiphilic stars, **CCS C5**−**6** and **CCS P1**−**3**, respectively, are provided in Figure 5. Saccharide-based amphiphilic star polymers **CCS C5** and **CCS C6** were prepared through 'click' attachment of monoazide functionalized $\beta$-galactopyranose and $\beta$-cyclodextrin onto **CCS 2**, with GPC-MALLS (DMF) revealing increases in $M_n$ from 267 kDa to 320 and 520 kDa, repectively. GPC RI chromatograms once again revealed peak shifts toward lower elution times (Figure 5a-b), possibly indicating an increase in the

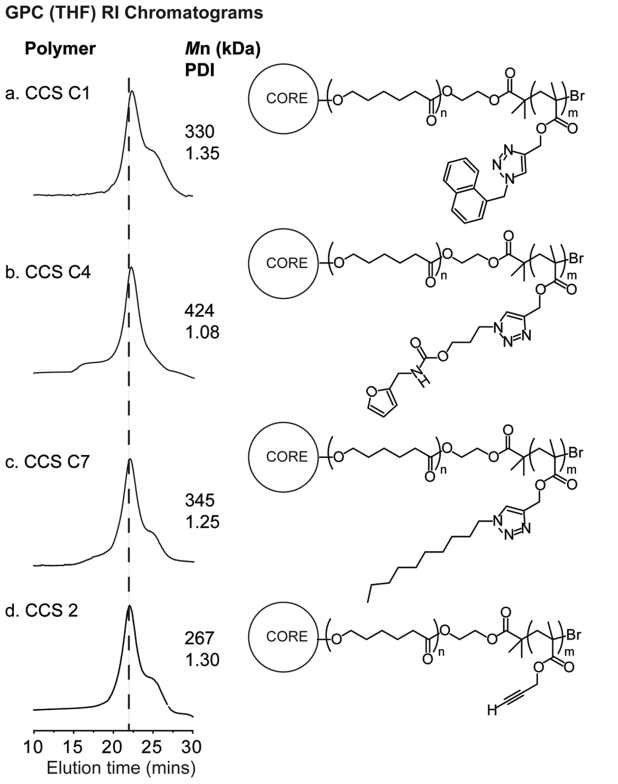


**Figure 6.** GPC (THF) RI chromatograms for quantitatively grafted CCS polymers: (a) naphthalene corona-functionalized star **CCS C1**, (b) furan corona-functionalized star **CCS C4**, (c) decane corona-functionalized star **CCS C7**, and (d) alkyne CCS polymer scaffold **CCS 2**.

structural rigidity as previously discussed. The successful click-functionalization of **CCS 2** with saccharide-based compounds **C5** and **C6** was also confirmed by $^1$H NMR spectroscopic analysis (Figure S6, Supporting Information) and DLS (Table 1).

Amphiphilic stars **CCS P1**−**3** were prepared by grafting various molecular weight azido substituted PEGs **P1**−**3**, respectively, allowing the effect of PEG degree of polymerization to be studied. In contrast to the saccharide functionalized stars, GPC RI analysis revealed a decrease in elution time for the PEG functionalized stars as a result of a large increase in molecular size, which was confirmed by DLS (Table 1). It is proposed that the long and flexible grafted PEG chains are capable of extending past the stars original alkyne corona, resulting in an increased molecular size without significantly increasing the overall structural rigidity. This would also be aided by any incompatibility between the inner shell PCL chains and grafted PEG.

**Synthesis of quantitatively grafted CCS polymers.** Out of all the CCS polymers functionalized via CuAAC chemistry, three displayed quantitative grafting efficiency, **CCS C1**, **CCS C4** and **CCS C7**. Whereas GPC RI chromatograms for these stars (Figure 6) revealed very slight peak shifts toward lower elution times, the $M_n$s closely resemble the theoretical molecular weights (100% grafting efficiency) (Table 1) within the determined margin of error. $^1$H NMR spectroscopic analysis (Table 1 and Figure S7, Supporting Information) also implied that quantitative click efficiency was achieved in agreement with GPC results. The high grafting efficiency can be accounted for by the small molecular size of compounds **C1**, **C4**, and **C7**, which minimizes steric hindrance and improves their ability to penetrate readily

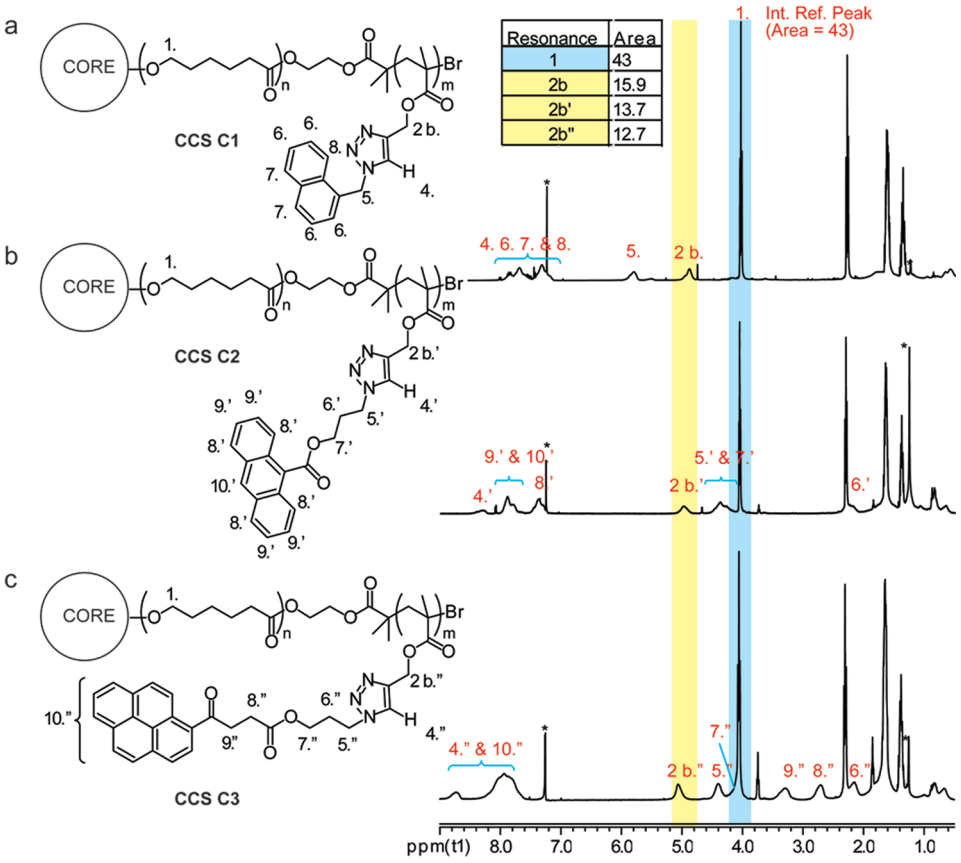


**Figure 7.** $^1$H NMR spectra of (**a**) naphthalene, (**b**) anthracene and (**c**) pyrene functionalized stars **CCS C1**, **CCS C2**, and **CCS C3**, respectively. The asterisk denotes solvent resonances.

into the corona of the star and access complementary reactive sites.

GPC RI chromatograms of **CCS C4** and **CCS C7** (Figure 6, b) displayed small shoulder peaks at low elution time ($t$ = 15−17 min), which are attributed to intermolecular coupling (i.e., star−star coupling) resulting from the previously discussed click side-reactions.

**Click Efficiency of High Density Functionalization of CCS Polymers.** Upon isolation, the click efficiency of the grafted CCS polymer was determined by $^1$H NMR spectroscopic analysis, using the integration of characteristic resonances (Figure 7, signals **1** and **2b**). For example, resonance **1** ($\delta_H$ = 4.05 ppm) corresponds to methylene protons adjacent to ester groups present along the backbone of the PCL arms, whereas resonance **2b** ($\delta_H$ = 5.05 ppm) results from methylene protons adjacent to triazoles formed through click reactions. For all click efficiency calculations resonance **1** was normalized to a value of 43, which corresponds to the average number of CL repeat units per arm. As such, the click efficiency can be calculated using the ratio of the area under resonance **2b** ($A_{2b}$) over the calculated alkyne repeated units ($N_{C\equiv C}$) per arm using eq 1, where $N_{C\equiv C}$ = 18 (Table S1, Supporting Information, entry 4). All calculated click efficiencies of various CCS polymers are summarized in Table 1.

$$CE = \frac{A_{2b}}{N_{C\equiv C}} \quad (1)$$

In contrast, the low click functionalization and difficulties in the separation of unreacted P$t$BA-N$_3$ precluded the use of $^1$H NMR spectroscopic analysis for determination of the click efficiency in the case of the P$t$BA functionalized star **CCS P4**. However, even without a good separation, the extent of click functionalization could be calculated from GPC, via integration and comparison of RI peak areas of the star and the unreacted P$t$BA-N$_3$ before and after reaction (Figure S8, Supporting Information).

The results obtained from click functionalization of the alkyne star **CCS 2** imply that the molecular size of the azido substituted compounds is a major factor affecting the click efficiency; the larger the molecular size of the azido substituted compounds, the lower the click efficiency. For example, NMR spectroscopic analysis of stars functionalized with **C1**, **C2**, and **C3**, revealed a decrease from 15.9 to 12.7 in the integrated area of the characteristic methylene resonance ($\delta_H$ = 5.05 ppm, **2b**, Figure 7), which indicates a decrease in the number of triazoles formed across these three reactions. This decrease in click efficiency can be explained by the increasing number of aromatic rings in going from **C1** to **C3**, which hinders the ability for the azido compounds to penetrate the stars' corona and reach the complementary alkyne functionalities. Therefore, the resultant CCS polymers are less functionalized when larger azido substituted compounds are employed. This is also supported by the series of PEG functionalized stars **CCS P1**−**3**, with the click efficiency decreasing as the degree of polymerization of the PEG-N$_3$ **P1**−**3** increased (Figure S9).

In order to gain a better understanding on the molecular size effect on the click efficiency of various azido compounds, the click efficiency versus estimated molecular size was plotted


dx.doi.org/10.1021/ma200283c |*Macromolecules* 2011, 44, 3189–3202

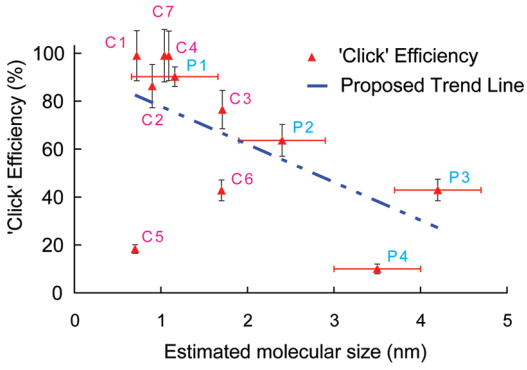


**Figure 8.** "Click" functionalization efficiency of azido substituted compounds onto the alkyne star **CCS 2** versus the estimated molecular size of those compounds.[62]

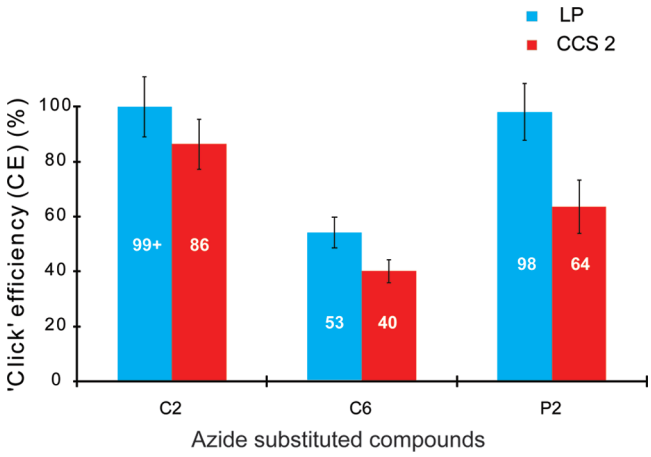


**Figure 9.** Bar chart comparing click functionalization efficiency of azido substituted compounds onto the alkyne star **CCS 2** and the linear macroinitiator **LP**.

(Figure 8). This graph clearly indicates there is a relationship between the click efficiency and the estimated size of the azido substituted compounds; a linear trend line with negative slope is included to illustrate this relationship. Evidently, terminal azido polymers with higher degrees of polymerization and larger molecular sizes (**P2**−**4**) displayed lower grafting efficiencies than azido substituted compounds (**C1**−**4**, **C6**, and **C7**) as a result of steric effects and entropic penalties.[54−57] Among the terminal azido polymers, P*t*BA-$N_3$ possessed the lowest click efficiency due to its bulky pendent tertiary butyl groups along the polymer chain and secondary azide, resulting in a high degree of steric hindrance. Interestingly, the $\beta$-galactopyranosyl azide **C5** revealed a large deviation from the proposed trend line. With an estimated molecular size of less than 1 nm, the low click efficiency (18%) of **C5** indicates that other factors in addition to the proposed size-efficiency relationship are responsible for its low click efficiency. For example, the hydrophilic nature of **C5** could lead to incompatibility issues with the hydrophobic alkyne CCS polymer, making it difficult for **C5** to approach and diffuse through the hydrophobic corona and react with the pendent alkynes, as has been reported for compounds with similar structures.[58] In addition, the secondary azide of **C5** attached directly to the sugar without any alkyl spacer between the azide group and the sugar ring would experience more steric restrictions than its primary azide counterparts resulting in decreased click efficiencies.

Contradictory to the proposed theory is the relatively high click efficiency of the monoazido $\beta$-CD **C6**, which is also comprised of hydrophilic sugars like **C5** and has a significantly larger molecular size. This unexpected result is believed to result from the hydrophobic internal cavity of **C6** and slightly lower hydrophilicity than **C5**, which allows **C6** to penetrate the corona of the hydrophobic star more readily. In addition, $\beta$-CDs can form unstable inclusion complexes[59−61] with hydrophobic moieties, such as the poly(propargyl methacrylate) repeat units of star **CCS 2**. This potential unstable inclusion complex formation would provide an additional synergistic driving force for **C6** to pass through and interact with the corona of the star to access the alkyne functionalities. Furthermore, the primary azide of **C6** makes it more reactive toward CuAAC chemistry, as opposed to the secondary azide of **C5**. So it is reasonable for **C6** to possess higher click efficiency than **C5**. On the other hand, comparing **C6** to the similarly sized azido pyrene **C3** reveals that the click efficiency of **C6** is still lower owing to its lower hydrophilicity-related incompatibility with the hydrophobic alkyne CCS polymer.

For CCS polymers, the arms are constrained within a compact sphere and assume a semidilute and random coil conformation at the inner and outer corona, respectively.[63] Limited space between adjacent arm polymers would hinder the diffusion of azido substituted compounds into the alkyne corona of the CCS polymer during click functionalization. In addition surrounding arms could shield the pendent alkyne groups away from the approaching azido compounds. Therefore, the click functionalization efficiency on the uncross-linked linear macroinitiator (arm precursor) would be expected to be higher than for the alkyne CCS polymer.

To demonstrate the effect of CCS architecture on click efficiency, the linear HO-P(CL-*b*-TMS-PgMA)-Br (Table S1, Supporting Information, entry 6) was deprotected and subsequently grafted with selected azide substituted compounds **C2**, **C6**, and **C7**. The click efficiency on the deprotected macroinitiator LP was calculated via $^1$H NMR spectroscopic analysis (Figures S10 and S11, Supporting Information) and compared with the click efficiency on **CCS 2** (Figure 9). The linear macroinitiator **LP 1** click efficiency was found to be ∼13, 13 and 34% higher than for the alkyne star **CCS 2** for compounds **C2**, **C6**, and **C7**, respectively. It is noteworthy that the click efficiency difference is less significant for polycyclic aromatic hydrocarbon **C2** and cyclic saccharide **C6** compared to the PEG-$N_3$ **P2**. The results reveal that the steric congestion generated by the arm conformation in the CCS polymer has less impact on the diffusion of small sized molecules (e.g., **C2** and **C6**) than macromolecules (e.g., **C7**).

## CONCLUSION

In this report, an improved synthetic approach toward the clickable alkyne CCS polymer scaffold was reported utilizing the robust stannous triflate ($Sn(OTf)_2$) catalyst for ring-opening polymerization. The reported approach provides high macroinitiator-to-star conversions and negligible star−star coupling, therefore increasing the yield of the alkyne CCS polymer. We have demonstrated that a library of highly corona-functionalized CCS polymers can be rapidly prepared by grafting the alkyne CCS polymer scaffold with various azido substituted compounds and polymers via CuAAC chemistry. For example, fluorescently tagged, saccharide-based and amphiphilic CCS polymers could

be readily prepared via the reported approach. However, in some cases the resulting functionalized CCS polymers suffer from an increase in molecular weight distribution due to star−star coupling caused by possible side-reactions of CuAAC chemistry. Through NMR spectroscopic analysis the number of click grafted compounds was quantified and ranged from 45 to 450 depending on their molecular size and functionality. The grafting efficiency (i.e., click efficiency) was studied for various azido substituted compounds and in general, it was found that small molecules with primary azide groups can be quantitatively grafted onto the alkyne CCS polymer via CuAAC chemistry. As the molecular size of the azide substituted compounds increase the click efficiency decreases. Terminal azido functionalized polymers can also be grafted onto the alkyne CCS polymer scaffold to afford stars with brush-like arms, although lower grafting efficiencies are observed due to steric hindrance and entropic penalties. An inversely related molecular size to click efficiency relationship was established, even though deviations from this proposed relationship still exist for some azido substituted compounds. These deviations can be explained by the hydrophilicity-related compatibility of functional compounds with the alkyne CCS scaffold, steric hindrance around the azide, and other synergic effects, such as the formation of potential inclusion complexes. Moreover, the steric congestion generated by the arm conformation within the CCS polymer results in lower click efficiency as compared to uncross-linked linear polymer (arm precursor). Therefore, this investigation has demonstrated that the high density functionalization of 3D nanostructures via the grafting-to approach is dependent on a number of factors and not just the molecular size of the functional compounds.

## ■ ASSOCIATED CONTENT

**Supporting Information.** Summary of macroinitiator "arm" synthesis, characterization results of macroinitiator **2** and **3**, "arm" number calculation of **CCS 1**, $^1$H NMR spectra of CCS polymer **CCS 1**, **2**, **C4**−**7** and **P1**−**3**, and grafted linear polymer **LP C2**, **C6** and **P2**, MALDI ToF MS spectra of terminal azido polymer **P1**−**4**, and DLS results of **CCS 2**, **C4**−**7** and **P1**−**3**, and fractional precipitation information. This material is available free of charge via the Internet at http://pubs.acs.org.

## ■ AUTHOR INFORMATION

### Corresponding Author

*E-mail: gregghq@unimelb.edu.au.

## ■ ACKNOWLEDGMENT

The authors wish to acknowledge the Australian Research Council (ARC Discovery Grant DP0986271) for financial support of this work. Jing M. Ren thanks Dr Zhiyuan Zhu for his valuable advice and suggestions.

## ■ REFERENCES

(1) Blencowe, A.; Tan, J. F.; Goh, T. K.; Qiao, G. G. *Polymer* **2009**, *50*, 5–32.
(2) Hadjichristidis, N. *J. Polym. Sci., Part A: Polym. Chem.* **1999**, *37*, 857–871.
(3) Wiltshire, J. T.; Qiao, G. G. *Aust. J. Chem.* **2007**, *60*, 699–705.
(4) Helms, B.; Guillaudeu, S. J.; Xie, Y.; McMurdo, M.; Hawker, C. J.; Fréchet, J. M. J. *Angew. Chem., Int. Ed.* **2005**, *44*, 6384–6387.
(5) Connal, L. A.; Qiao, G. G. *Adv. Mater.* **2006**, *18*, 3024–3028.
(6) Ho, A. K.; Iin, I.; Gurr, P. A.; Mills, M. F.; Qiao, G. G. *Polymer* **2005**, *46*, 6727–6735.
(7) Bae, Y.; Kataoka, K. *Adv. Drug Delivery Rev.* **2009**, *61*, 768–784.
(8) He, E.; Yue, C.; Tam, K. *J. Pharm. Sci.* **2010**, *99*, 782–793.
(9) Bencherif, S. A.; Gao, H.; Srinivasan, A.; Siegwart, D. J.; Hollinger, J. O.; Washburn, N. R.; Matyjaszewski, K. *Biomacromolecules* **2009**, *10*, 1795–1803.
(10) Ishikawa, A.; Zhou, Y.-M.; Kambe, N.; Nakayama, Y. *Bioconjugate Chem.* **2008**, *19*, 558–561.
(11) Matyjaszewski, K.; Xia, J. *Chem. Rev.* **2001**, *101*, 2921–2990.
(12) Kamigaito, M.; Ando, T.; Sawamoto, M. *Chem. Rev.* **2001**, *101*, 3689–3746.
(13) Hadjichristidis, N.; Iatrou, H.; Pitsikalis, M.; Sakellariou, G. *Chem. Rev.* **2009**, *109*, 5528–5578.
(14) Bielawski, C. W.; Grubbs, R. H. *Prog. Polym. Sci.* **2007**, *32*, 1–29.
(15) Stridsberg, K.; Ryner, M.; Albertsson, A.-C. In *Degradable Aliphatic Polyesters*; Springer: Berlin and Heidelberg, Germany: 2002; Vol. 157, p 41−65.
(16) Sulistio, A.; Widjaya, A.; Blencowe, A.; Zhang, X.; Qiao, G. *Chem. Commun.* **2011**, *47*, 1151–1153.
(17) Baek, K.-Y.; Kamigaito, M.; Sawamoto, M. *Macromolecules* **2001**, *34*, 7629–7635.
(18) Xia, J.; Zhang, X.; Matyjaszewski, K. *Macromolecules* **1999**, *32*, 4482–4484.
(19) Connal, L. A.; Vestberg, R.; Hawker, C. J.; Qiao, G. G. *Macromolecules* **2007**, *40*, 7855–7863.
(20) Connal, L. A.; Li, Q.; Quinn, J. F.; Tjipto, E.; Caruso, F.; Qiao, G. G. *Macromolecules* **2008**, *41*, 2620–2626.
(21) Deming, T. J. *J. Polym. Sci., Part A: Polym. Chem.* **2000**, *38*, 3011–3018.
(22) Sumerlin, B. S.; Tsarevsky, N. V.; Louche, G.; Lee, R. Y.; Matyjaszewski, K. *Macromolecules* **2005**, *38*, 7540–7545.
(23) Quémener, D.; Le Hellaye, M.; Bissett, C.; Davis, T. P.; Barner-Kowollik, C.; Stenzel, M. H. *J. Polym. Sci., Part A: Polym. Chem.* **2008**, *46*, 155–173.
(24) Ohno, K.; Tsujii, Y.; Fukuda, T. *J. Polym. Sci., Part A: Polym. Chem.* **1998**, *36*, 2473–2481.
(25) Ishitake, K.; Satoh, K.; Kamigaito, M.; Okamoto, Y. *Angew. Chem., Int. Ed.* **2009**, *48*, 1991–1994.
(26) Wiltshire, J. T.; Qiao, G. G. *J. Polym. Sci., Part A: Polym. Chem.* **2009**, *47*, 1485–1498.
(27) Rostovtsev, V. V.; Green, L. G.; Fokin, V. V.; Sharpless, K. B. *Angew. Chem.* **2002**, *114*, 2708–2711.
(28) Wang, Q.; Chan, T. R.; Hilgraf, R.; Fokin, V. V.; Sharpless, K. B.; Finn, M. G. *J. Am. Chem. Soc.* **2003**, *125*, 3192–3193.
(29) Tornøe, C. W.; Christensen, C.; Meldal, M. *J. Org. Chem.* **2002**, *67*, 3057–3064.
(30) Wiltshire, J. T.; Qiao, G. G. *Macromolecules* **2006**, *39*, 4282–4285.
(31) Wiltshire, J. T.; Qiao, G. G. *Macromolecules* **2006**, *39*, 9018–9027.
(32) Malkoch, M.; Thibault, R. J.; Drockenmuller, E.; Messerschmidt, M.; Voit, B.; Russell, T. P.; Hawker, C. J. *J. Am. Chem. Soc.* **2005**, *127*, 14942–14949.
(33) Derouet, D.; Forgeard, S.; Brosse, J. *Macromol. Chem. Phys.* **1998**, *199*, 1835–1842.
(34) Sirion, U.; Kim, H. J.; Lee, J. H.; Seo, J. W.; Lee, B. S.; Lee, S. J.; Oh, S. J.; Chi, D. Y. *Tetrahedron Lett.* **2007**, *48*, 3953–3957.
(35) Ohga, K.; Takashima, Y.; Takahashi, H.; Kawaguchi, Y.; Yamaguchi, H.; Harada, A. *Macromolecules* **2005**, *38*, 5897–5904.
(36) Takahashi, K.; Hattori, K.; Toda, F. *Tetrahedron Lett.* **1984**, *25*, 3331–3334.
(37) Zhong, N.; Byun, H.-S.; Bittman, R. *Tetrahedron Lett.* **1998**, *39*, 2919–2920.

(38) Petter, R. C.; Salek, J. S.; Sikorski, C. T.; Kumaravel, G.; Lin, F. T. *J. Am. Chem. Soc.* **1990**, *112*, 3860–3868.
(39) Davis, K. A.; Matyjaszewski, K. *Macromolecules* **2000**, *33*, 4039–4047.
(40) Braunecker, W. A.; Pintauer, T.; Tsarevsky, N. V.; Kickelbick, G. *J. Organomet. Chem.* **2005**, *690*, 916–924.
(41) Braunecker, W. A.; Tsarevsky, N. V.; Pintauer, T.; Gil, R. R.; Matyjaszewski, K. *Macromolecules* **2005**, *38*, 4081–4088.
(42) Möller, M.; Kånge, R.; Hedrick, J. L. *J. Polym. Sci., Part A: Polym. Chem.* **2000**, *38*, 2067–2074.
(43) Möller, M.; Nederberg, F.; Lim, L. S.; Kånge, R.; Hawker, C. J.; Hedrick, J. L.; Gu, Y.; Shah, R.; Abbott, N. L. *J. Polym. Sci., Part A: Polym. Chem.* **2001**, *39*, 3529–3538.
(44) Goh, T. K.; Yamashita, S.; Satoh, K.; Blencowe, A.; Kamigaito, M.; Qiao, G. G. *Macromol. Rapid Commun.* **2011**, *32*, 456–461.
(45) Burdyńska, J.; Cho, H. Y.; Mueller, L.; Matyjaszewski, K. *Macromolecules* **2010**, *43*, 857–871.
(46) Lin, W.; Fu, Q.; Zhang, Y.; Huang, J. *Macromolecules* **2008**, *41*, 4127–4135.
(47) Balk, S.; Loehden, G.; Miess, C.; Troemer, C.; Maerz, M.; WO Patent WO/2007/115,848: 2007.
(48) Polymer standards are tested with the GPC systems using the known d*n*/d*c* values or the known injected mass of polymer sample based on the assumption of 100% mass recovery from the GPC RI chromatogram. The determined molecular weight results of the polymer standards determined by both methods are in good agreement with slight difference within error margin. See the following references for similar methods used:(a) Kim, Y. S.; Kadla, J. F. *Biomacromolecules* **2010**, *11*, 981–988. (b) Wiltshire, J. T.; Qiao, G. G. *J. Polym. Sci., Part A: Polym. Chem.* **2009**, *47*, 1485–1498. (c) Li, W.; Matyjaszewski, K. *J. Am. Chem. Soc.* **2009**, *131*, 10378–10379.
(49) Duxbury, C. J.; Cummins, D.; Heise, A. *J. Polym. Sci., Part A: Polym. Chem.* **2009**, *47*, 3795–3802.
(50) Laurent, B. A.; Grayson, S. M. *J. Am. Chem. Soc.* **2006**, *128*, 4238–4239.
(51) Abdel-Mottaleb, M. S.; Galal, H. R.; Dessouky, A. F. M.; El-Naggar, M.; Mekkawi, D.; Ali, S. S.; Attya, G. M. *Int. J. Photoenergy* **2000**, *2*, 47–53.
(52) Atherton, J. C. C.; Jones, S. *Tetrahedron* **2003**, *59*, 9039–9057.
(53) Bouas-Laurent, H.; Desvergne, J. P.; Castellan, A.; Lapouyade, R. *Chem. Soc. Rev.* **2000**, *29*, 43–55.
(54) Lammens, M.; Fournier, D.; Fijten, M. W. M.; Hoogenboom, R.; Du Prez, F. *Macromol. Rapid Commun.* **2009**, *30*, 2049–2055.
(55) Ternat, C.; Kreutzer, G.; Plummer, C. J. G.; Nguyen, T. Q.; Herrmann, A.; Ouali, L.; Sommer, H.; Fieber, W.; Velazco, M. I.; Klok, H. A. *Macromol. Chem. Phys.* **2007**, *208*, 131–145.
(56) Gungor, E.; Durmaz, H.; Hizal, G.; Tunca, U. *J. Polym. Sci., Part A: Polym. Chem.* **2008**, *46*, 4459–4468.
(57) Altintas, O.; Hizal, G.; Tunca, U. *J. Polym. Sci., Part A: Polym. Chem.* **2006**, *44*, 5699–5707.
(58) Dedola, S.; Hughes, D. L.; Nepogodiev, S. A.; Rejzek, M.; Field, R. A. *Carbohyd. Res.* **2010**, *345*, 1123–1134.
(59) Madison, P. H.; Long, T. E. *Biomacromolecules* **2000**, *1*, 615–621.
(60) Deng, J.; Wu, Z.; He, Q.; Yang, W. *Polym. Adv. Technol.* **2008**, *19*, 1649–1655.
(61) Glöckner, P.; Ritter, H. *Macromol. Chem. Phys.* **2000**, *201*, 2455–2457.
(62) Molecular modelling and size estimation were implemented using ChemDraw Ultra (version 12.0). All structures were optimized with MM2 to minimize steric energy. For polymers, random coil conformations were adopted.
(63) Goh, T. K.; Coventry, K. D.; Blencowe, A.; Qiao, G. G. *Polymer* **2008**, *49*, 5095–5104.